Mineralium Deposita
https://doi.org/10.1007/s00126-022-01122-2

ARTICLE

Porphyry-epithermal Cu-Mo-Au–Ag mineralization in the Nakhodka ore field, Baimka Trend, Chukotka, Russia: a geological, mineralogical, and geochemical perspective

Andrey F. Chitalin[1] · Ivan A. Baksheev[2] · Yurii N. Nikolaev[2] · Ekaterina V. Nagornaya[2,3] · Yuliya N. Khabibullina[2] · Irina Yu. Nikolaeva[2] · Ildar A. Kalko[2] · Daniel Müller[4]

Received: 22 November 2021 / Accepted: 6 May 2022

Abstract

The Nakhodka ore field (NOF) is situated in the Baimka Trend, Chukotka, Russia, and comprises the Vesenny epithermal Au–Ag, and Malysh, Nakhodka, Vesenny III, and Pryamoy porphyry Cu-Au ± Mo deposits. Porphyry and epithermal mineralization of the NOF are hosted by Early Cretaceous diorite and monzonite intrusions, which are dated at 139–141 Ma (U–Pb zircon). The NOF mineralization is structurally controlled. The prevailing stress field during the evolution in the Baimka dextral shear zone (also known as Baimka Trend) has led to the formation of extensional and strike-slip structures that control distinct zones with strong quartz-sericite alteration and sheeted high-grade quartz–sulfide veining; characteristics that are similar to the world-class Peschanka porphyry Cu-Au deposit located about 20 km to the NW of the NOF. Four types of hydrothermal alteration are documented in the NOF: (1) potassic, (2) propylitic, (3) quartz-sericite, and more rarely (4) argillic. Two phases of porphyry-style mineralization are distinguished: (1) early-stage quartz-magnetite veining associated with potassic alteration and (2) sheeted quartz-sulfide (bornite, chalcopyrite, molybdenite, pyrite) veining that is spatially associated with a strong quartz-sericite alteration assemblage. Epithermal Au–Ag mineralization belongs to the intermediate-sulfidation type and consists of gold-bearing polymetallic quartz-dolomite ± rhodochrosite veins and veinlets. The NOF is defined by a distinct geochemical zonation. Geophysical data show that the high-grade stockwork zones at the Vesenny III porphyry Cu-Au deposit are defined by pronounced magnetic anomalies reflecting abundant hydrothermal magnetite veining, while the Vesenny epithermal Au–Ag deposit is defined by a strong negative magnetic anomaly due to strong silicification and magnetite-destructive quartz-sericite to argillic alteration.

Keywords Porphyry Cu-Au · Epithermal Au–Ag mineralization · Nakhodka ore field · Baimka Trend · Chukchi Peninsula · Russia

Introduction

The Chukotka region in North-East Russia, comprises the Baimka Trend, a well-endowed mineral belt located about 200 km to the southwest of the town of Bilibino. The Baimka Trend includes a cluster of porphyry Cu-Au and epithermal Au–Ag projects (Fig. 1). The most advanced exploration project to date is Peschanka (also known as Baimskaya), which crops out at surface and is well defined by systematic deep diamond drilling (Chitalin et al. 2012, 2013, 2021).

Peschanka represents the largest porphyry Cu-Au ± Mo deposit in Russia, comprising a JORC resource of > 9.5 Mt Cu with an ore grade of 0.43% Cu and > 16.5 Moz Au with an ore grade of 0.23 g/t Au (kazminerals.com); it ranks among the top 10 undeveloped greenfield copper projects

Editorial handling: B. Lehmann

✉ Ivan A. Baksheev
ivan.baksheev@gmail.com

1 Institute of Geotechnology, Moscow State University, Science Park 1, Leninskie Gori, Moscow 119234, Russia

2 Faculty of Geology, Lomonosov Moscow State University, GSP-1, Leninskie Gory, Moscow 119991, Russia

3 Vernadsky Institute of Geochemistry and Analytical Chemistry Russian Academy of Sciences, 19 Kosygin str., Moscow 119991, Russia

4 Santiago, Chile

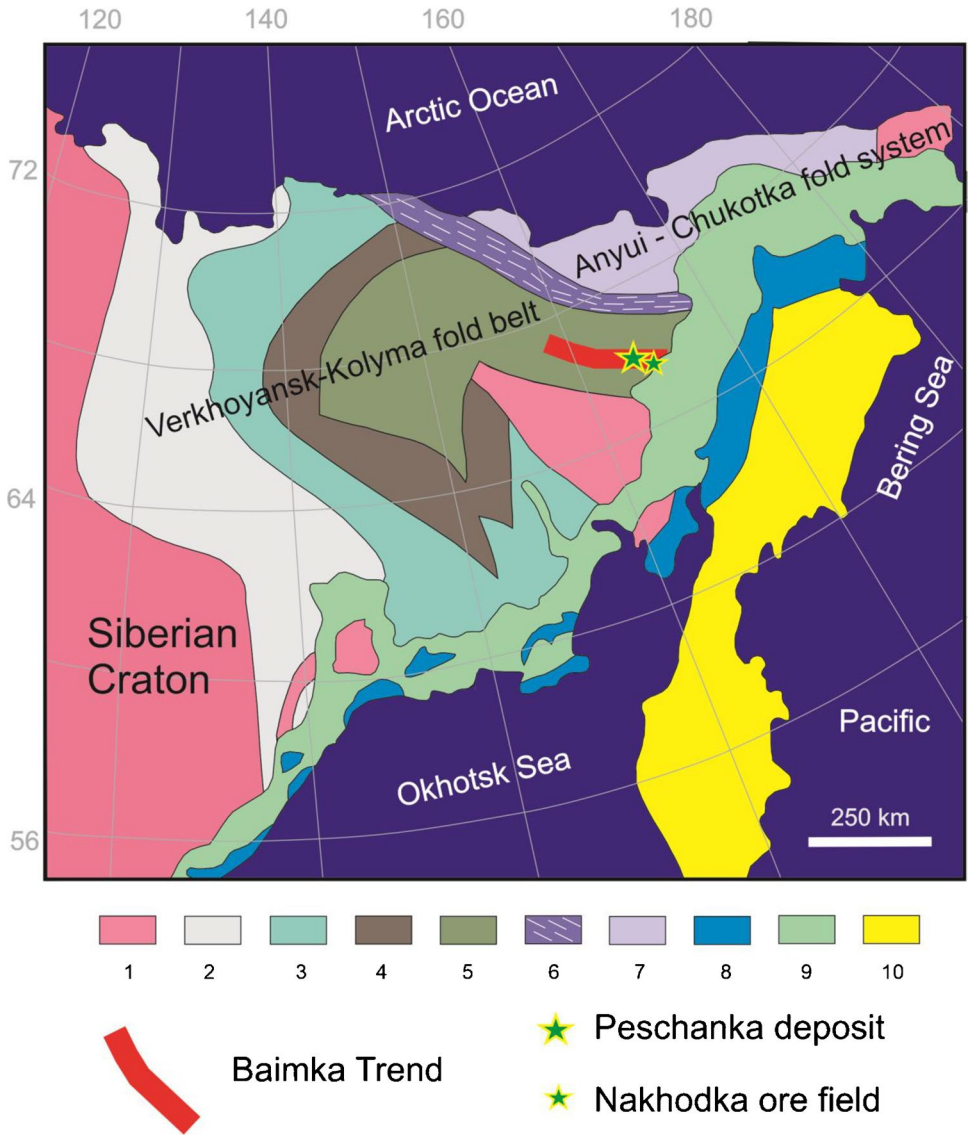

Fig. 1 Tectonic sketch map of northeastern Russia (simplified after Sokolov 2010) showing the location of the Baimka Trend and related porphyry-Cu-Au deposits: (1) Siberian Craton and cratonic terranes; (2) Verkhoyansk terrane; (3) Yana-Kolyma terrane; (4) Paleozoic terranes; (5) Alazeya-Oloy fold system; (6) South-Anyui Suture; (7) East Chukotka terrane; (8) Late-Jurassic magmatic belt; (9) Okhotsk-Chukotka Cretaceous magmatic belt; and (10) Koryak-Kamchatka fold belt, respectively

worldwide. Peschanka is an example of copper–gold mineralization hosted by potassic intrusions with high oxidation state, comparable to Grasberg, Indonesia (Pollard and Taylor 2001); Oyu Tolgoi, Mongolia (Crane and Kavalieris 2012); and Pebble, Alaska (Olson et al. 2017). It probably also represents the most isolated copper–gold deposit of significant grade and tonnage worldwide (Chitalin et al. 2012, 2021; Marushchenko et al. 2015, 2018).

The Nakhodka ore field (NOF) is another economically significant hydrothermal Cu-Mo-Au–Ag system in the Baimka Trend (Fig. 1). It is located about 20 km SE of Peschanka and includes the Vesenny porphyry-epithermal Au–Ag, and the Malysh, Nakhodka, Vesenny III, and Pryamoy porphyry Cu-Au ± Mo deposits. The inferred JORC compliant mineral resource of the combined Nakhodka and Pryamoy deposits is estimated by IMC Montan (Cu_{Eq} cut-off grade of 0.3%) totaling about 918 Mt of ore, including 3.1 Mt of Cu, 50 kt Mo, 9 Moz of Au, and 37 Moz of Ag at average grades of 0.34% Cu, 0.0054% Mo, 0.30 g/t Au, and 1.2 g/t Ag, respectively. The Vesenny epithermal precious-metal deposit consists of two orebodies: (1) high-grade veining with about 4.38 Mt of ore, including 0.5 Moz of gold and 4.5 Moz of silver at average grades of 3.4 g/t Au and 31.4 g/t Ag, respectively, and (2) stockwork mineralization containing about 65.74 Mt of ore, including > 3 Moz of Au and 30 Moz of Ag at average grades of 1.48 g/t Au and 13.6 g/t Ag (Chitalin et al. 2013), using a gold equivalent cut-off grade of about 1 g/t. The district has only partially been explored and still holds significant upside potential (Chitalin et al. 2019).

Both the Peschanka deposit and the NOF were discovered during a scout drilling program during the late-1970s and 1980s. Follow-up exploration was carried out during the period of 2009–2019 by the Baimka Mining Company and

under guidance of the Regional Mining Company, LLC. In late 2019, KAZ Minerals acquired the Pechanka/Baimskaya copper project and commenced with the 8.5 billion USD mine development. Due to the high exploration potential for additional satellite porphyry Cu-Au orebodies, KAZ Minerals also conducts an extensive brownfields exploration program including the NOF (Chitalin et al. 2021).

This paper provides an overview of the tectonic setting, structural framework, hydrothermal alteration, and mineralization styles of the Nakhodka porphyry-epithermal deposit cluster and presents new mineralogical, geochemical, and geophysical data.

Regional and local geology

The West Chukotka area consists of four major tectonomagmatic elements, from the SW to the NE (Fig. 2): (1) the Omolon cratonic terrane; (2) the Oloy zone, dominated by Jurassic and Early Cretaceous continental-arc magmatism; (3) the South Anyui Suture formed during the Early Cretaceous and after the closure of the oceanic basin by subsequent collision between the Chukotka block and the Siberian craton, and (4) the Anyui zone, representing the former passive margin of the Chukotka block (Parfenov 1991; Nokleberg et al. 2000). All four zones are overprinted by a post-collisional magmatic event dated at about 121–112 Ma (Tikhomirov et al. 2017; Kara et al. 2019; Nagornaya et al. 2020) and, subsequently, by subduction-related volcanism along the Okhotsk-Chukotka volcanic belt dated at about 106–74 Ma (Akinin and Miller 2011; Tikhomirov et al. 2012).

The Oloy tectonic zone includes the Baimka Trend, which hosts the world-class Peschanka and Nakhodka porphyry Cu-Au ± Mo deposits as well as several smaller porphyry Cu-Au and epithermal Au prospects (Chitalin et al. 2021). The Baimka Trend has a NW-strike with a length of approximately 200 km and a width ranging from 25 to 50 km. It is structurally controlled by the regional Baimka Shear Zone (Fig. 3; Chitalin et al. 2013, 2016). All mineral deposits and occurrences are spatially associated with high-K monzonite intrusions of the Early Cretaceous Egdykgych Complex.

The Baimka Shear Zone was formed in two stages during the Late Jurassic to Early Cretaceous (Chitalin 2019a). During the initial stage, the Upper Jurassic volcanic and volcano-sedimentary sequences were folded, and NW-trending sinistral strike-slip and reverse faults formed in relation to a regional left-lateral shear system (Fig. 3). The Early Cretaceous composite Egdykgych plutonic complex intruded along these faults and was subsequently cut and displaced along the NW-trending reactivated dextral strike-slip fault. The second phase is documented by secondary extensional structures, normal faults and strike-slip faults, respectively. Extensional structures within this large shear zone controlled the emplacement of the Early Cretaceous intrusions and the formation of porphyry Cu-Au ± Mo deposits. Gold-bearing epithermal veins and sheeted vein zones mainly developed along dextral strike-slip and conjugated sinistral strike-slip faults.

At the Peschanka north flank, mineralized rocks are unconformably overlain by post-mineral sedimentary rocks of the Late Aptian Ainakhkurgen Formation (Chitalin et al. 2022). The Late Cretaceous basalt and andesite dikes are the youngest rocks in the Baimka area, apart from local Quaternary alluvial cover sequences. Strike-slip movements and associated thrust faults were active at least until the Albian. Cenozoic low-angle thrust faults with cataclastic textures intersect the stockwork veining at the Nakhodka porphyry Cu-Au deposit (Chitalin et al. 2016; Chitalin 2019a).

Nakhodka ore field geology

The Nakhodka ore field is located in the southern part of the partly eroded Early Cretaceous Upper Baimka diorite complex (Fig. 4). This composite stock consists of two diorite and quartz-diorite porphyry phases, which are locally intruded by small monzodiorite and quartz-monzonite porphyry plugs that belong to the Early Cretaceous Egdygkych pluton. All intrusions intersect the folded Upper Jurassic volcano-sedimentary sequences as well as Late Jurassic gabbroic to dioritic stocks and dykes. The U–Pb zircon ages of quartz-diorite and quartz-monzodiorite porphyries of the Nakhodka ore field yield about 139–141 Ma (Fig. 4 and ESM 1). Post-mineral Late Cretaceous andesite and basalt dykes post-date and cut all other units and mineralized structures (Chitalin et al. 2013, 2014, 2016, 2019; Marushchenko et al. 2018).

The porphyry-type Cu-Au mineralization predominantly occurs at the margins of the Upper Baimka stock forming wide linear mineralized zones. Significant porphyry Cu-Au ± Mo mineralization is recorded at the Nakhodka porphyry Cu-Au deposit as well as at Vesenny III, and the eastern flank of the Pryamoy deposit (Fig. 4). Porphyry Cu-Au ± Mo mineralization at the Nakhodka deposit is confirmed to vertical depths of at least 600 m below surface, but remains open at depth. Minor sub-economic porphyry Cu occurrences are exposed at the western flank of the Upper Baimka stock and were intersected in exploration drillholes in the vicinity of the Vesenny epithermal Au–Ag deposit (Fig. 4). Copper-poor but Mo-rich porphyry-type mineralization is recorded both at the Malysh and the western flank of the Pryamoy deposit (Fig. 4). The Re-Os molybdenite age of 137.9 ± 0.3 Ma (ESM 1) is consistent with the U–Pb

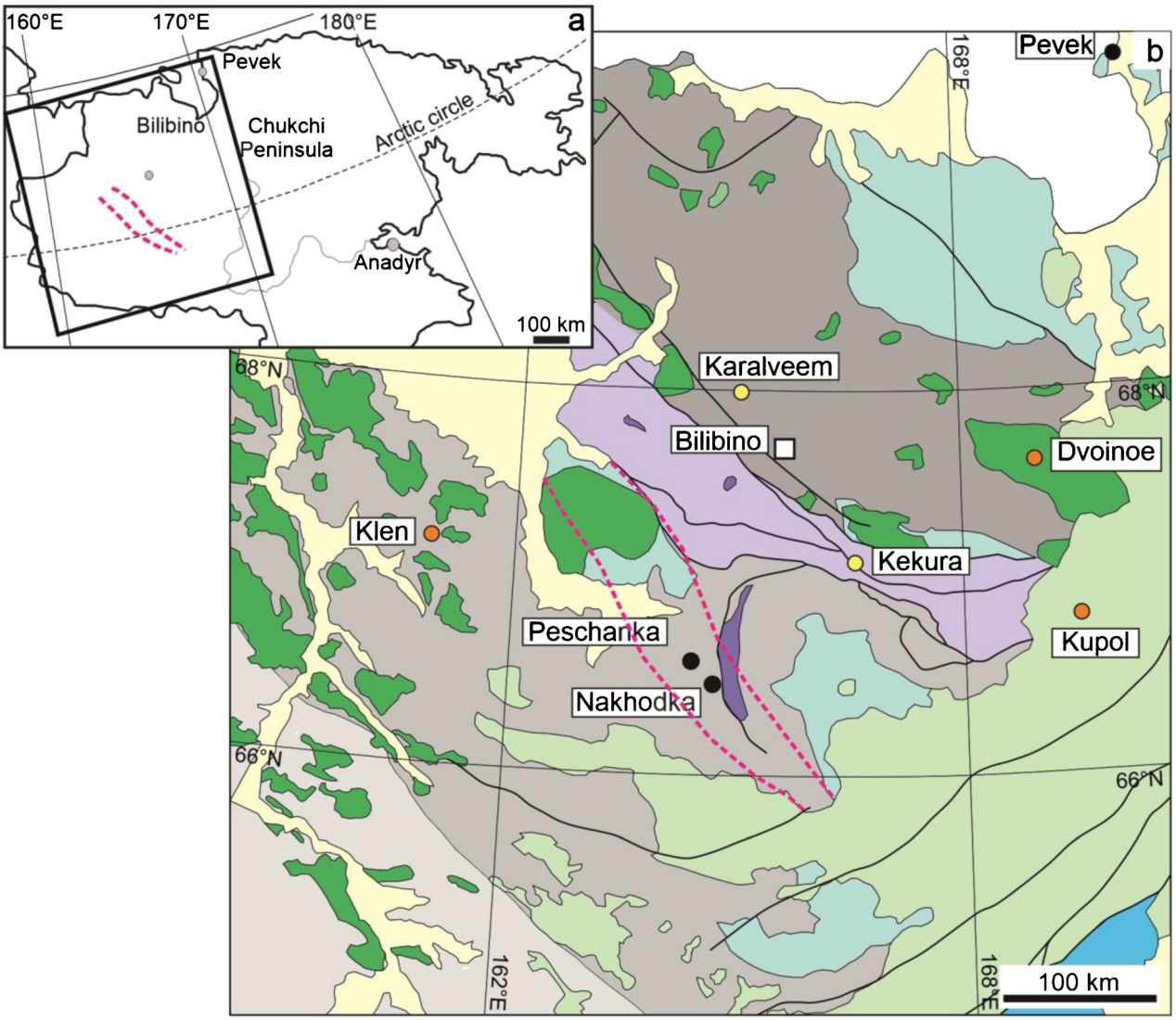

Tectonic zones of the Verkhoyansk-Chukotka province

- Omolon (a slightly deformed cover of Paleozoic and Mesozoic clastic and volcanic strata over the Precambrian crystalline basement)
- Oloy (tectonic collage of Paleozoic and Mesozoic active margin complexes)
- South Anyui (suture zone formed after the closure of an oceanic basin; strongly deformed Mesozoic clastic and volcanic strata)
- Anyui (Late Permian(?) through Triassic clastic complexes of the passive margin of Chukotka continental block)
- Late Jurassic through Early Cretaceous syn-collisional and post-collisional basins filled with clastic sediments
- Massifs of Paleozoic ophiolitic gabbro and peridotites
- Baimka Trend

- Aptian volcanic complexes
- Uda-Murgal belt (Late Jurassic through Early Cretaceous)
- Okhotsk-Chukotka belt (Albian through Campanian)

Subduction-related volcanic belts

- Quaternary sediments
- Major faults
- Porphyry Cu-Mo-Au deposit
- Au granitoid-related deposit
- Au-Ag IS / LS epithermal deposit

◂**Fig. 2** Geographical location of the Baimka Trend (**a**) and tectonic map of Western Chukotka (**b**), modified after Tikhomirov et al. (2017) and Chitalin et al. (2021)

zircon dating and confirms the genetic relationship between hydrothermal mineralization and the high-K intrusions of the Egdykgych Complex (Nagornaya 2013).

The Nakhodka porphyry Cu-Au ± Mo deposit includes a north–south striking mineralized corridor, up to 300 m thick, and steeply dipping to the east (Figs. 5 and 6). Figure 6a illustrates the typical metal zonation of the porphyry system consisting of a bornite-rich core with the highest Cu contents, which grades outwards into a chalcopyrite-dominated zone surrounded by a pyrite shell. Chitalin et al. (2016) document that an initial porphyry Mo stage pre-dates the main porphyry Cu-Au mineralization at Nakhodka. The Cu-rich porphyry-style mineralization at the Nakhodka deposit as well as the Vesenny III and Pryamoy deposits forms en-echelon subvertical N-S trending quartz-sulfide lenses and multiple zones with intense stockwork veining that are spatially associated with strong quartz-sericite alteration (Fig. 5a and c and ESM 2, 3). In places, there are also N-S oriented hydrothermal breccias, which cut the early-stage porphyry Cu-Au ± Mo mineralization (Figs. 5b, 6b, and 7b and ESM 4).

Telescoping in the NOF comprises two main phases: (1) porphyry Cu-Au ± Mo mineralization (Figs. 5c and 6) and (2) an intermediate-sulfidation (IS) epithermal Au assemblage (Figs. 5c and 7b). Locally, Au-bearing banded quartz-carbonate veins and ENE-WSW trending vein zones (linear stockworks) cut the early-stage porphyry Cu-Au ± Mo mineralization and hydrothermal breccias (Figs. 6 and 7 and ESM 5).

In places, the porphyry-style mineralization is intersected by post-mineral sinistral and dextral strike-slip faults, with lateral offsets of up to 1 km. Telescoping by overprinting phases of epithermal Au–Ag mineralization is evident at all porphyry-style deposits and occurrences of the NOF, but most intensely at the Vesenny and Pryamoy deposits (Fig. 5c).

The structural setting and orientation of mineralized veining in the NOF are documented in detail by Chitalin et al. (2014) and discussed by Chitalin et al. (2016, 2019, 2020) and Chitalin (2019a, b, 2021). Mineralized quartz-sulfide veining is commonly associated with strong quartz-sericite alteration at the Nakhodka porphyry Cu-Au deposit as well as the Vesenny III deposit (Figs. 8 and 9 and ESM 3, 6, 7). Zones of quartz-sericite alteration typically trend NW (Fig. 8c), but quartz veining predominantly strikes NS cross-cutting these zones. However, there are local zones with stockwork mineralization and the main vein orientations are N-S and E-W, respectively (Fig. 8d). Sulfide disseminations and veinlets locally overprint both quartz veining and quartz-sericite alteration zones. At the same time, irregularly distributed unmineralized quartz veining and quartz-sericite alteration are also recorded.

Mineralized fractures and veins include strike-slip, reverse, and extensional structures (ESM 8). Copper, Au, and Mo are hosted by quartz stockwork veining (ESM 9). The evolution of the Vesenny porphyry Cu-Mo and epithermal Au–Ag deposit is rather complex (Fig. 10a). At Vesenny, different types of hydrothermal alteration such as propylitic, quartz-sericite, and potassic assemblages as well as hydrothermal breccias are structurally controlled and spatially associated with porphyry-style Cu-Mo mineralization. Subsequent telescoped intermediate-sulfidation epithermal Au–Ag-bearing quartz-carbonate veins overprint the early-stage porphyry Cu-Mo mineralization. Epithermal veins and veinlets are documented by exploration drilling to vertical depths of at least 450 m (Chitalin et al. 2013, 2016). Structural stereograms illustrating the complex structural setting of Vesenny and its structurally controlled quartz-sericite alteration zones as well as epithermal quartz-carbonate veining are shown in Fig. 10b.

A stereogram synthesizing all unmineralized fractures, both pre- and post-mineralization, recorded in NOF is shown in ESM 10. The four main structural orientations are NW, NE, S–N, and W-E. The pole *maxima* form an arc of a small circle nearly consistent with the projection of the great circle of the stereogram base which is typical of strike-slip faults and associated structures forming in a so called "shear stress field" or "wrench regime" by horizontal principal stresses σ1 (compression) and σ3 (extension). The pole *maxima* also form belts of small circles with a vertical axis (ESM 10b and c). They are interpreted as contraction cracks in the roof zone of the diorite stock. During horizontal compression in the shear stress field, some of these cracks were opened and filled with hydrothermal fluids (mineralized cracks). In other words, we suggest that mineralizing fluids were emplaced into available fracture systems, rather than formed as a result of fluid overpressure.

A 3-D model of the porphyry Cu-Mo mineralization and epithermal Au–Ag overprint in the NOF is illustrated in Fig. 11. Note that Mo- and Cu-bearing stockwork zones commonly broadly overlap, except at the Malysh deposit, which is a Mo-dominant porphyry system. The orientation of veins and veining zones is controlled by local extensional structures in the shear zone (Fig. 12a), similar to the Peschanka porphyry Cu-Au-Mo deposit (Chitalin et al. 2012). Epithermal veins and veining zones at the Nakhodka ore field are interpreted as local extensional en-echelon structures within the conjugate shear zones (Fig. 12b; Chitalin 2021; Chitalin et al. 2016, 2019).

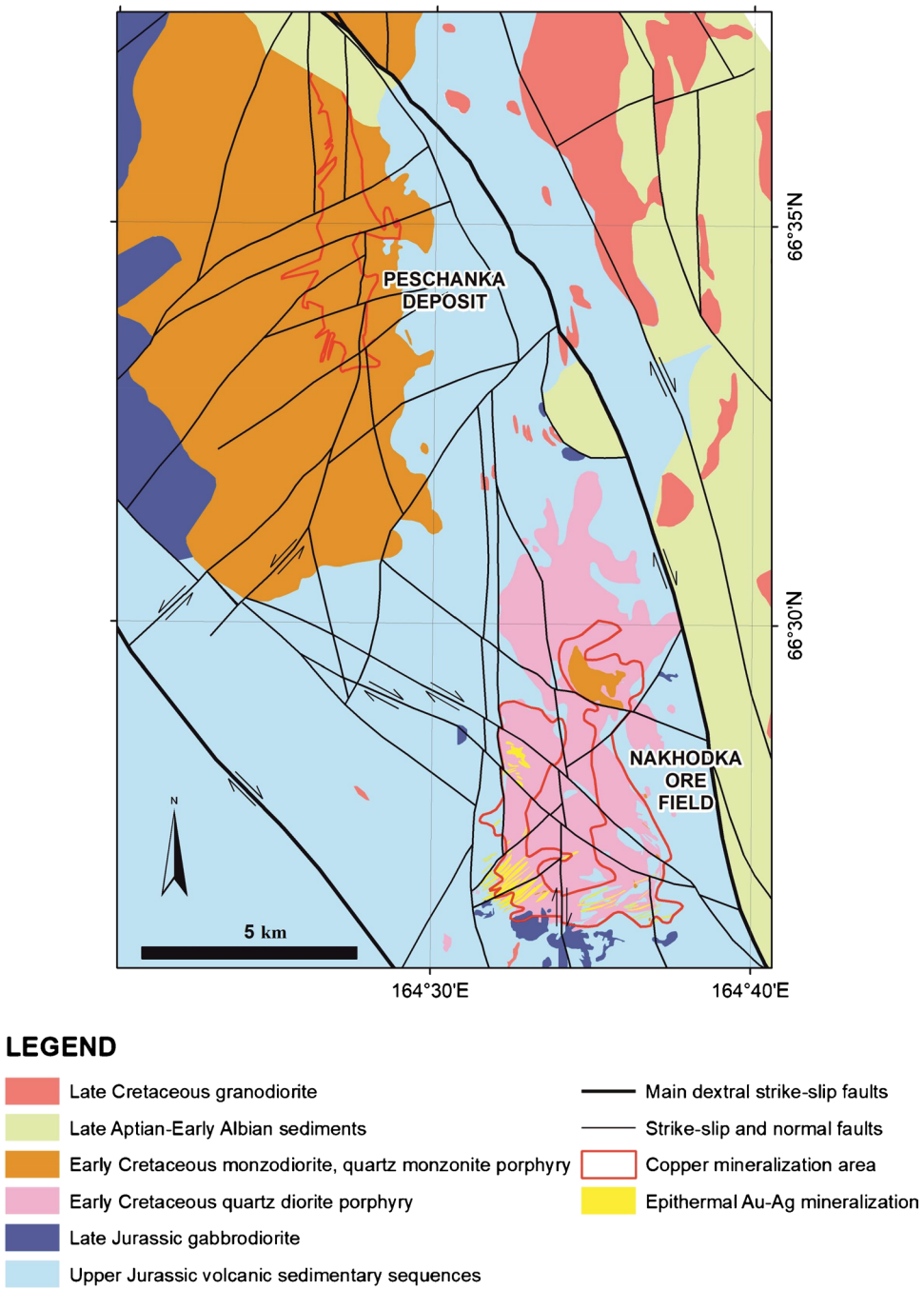

Fig. 3 Geological and mineralization sketch map of the Baimka Trend central part

Hydrothermal alteration in the Nakhodka ore field

The Nakhodka intrusions are overprinted by wide-spread hydrothermal alteration including potassic (biotite-magnetite-potassium feldspar-quartz), propylitic (chlorite-epidote-actinolite-albite-calcite), quartz-sericite (quartz-sericite-pyrite-carbonate) assemblages as well as zones of pervasive silicification and, less commonly, argillic alteration assemblages (Fig. 5 and ESM 2).

Potassic alteration is rarely exposed at the surface, but very common in drill core, usually overprinting the monzodiorite stocks (Figs. 6 and 7). By contrast, sheeted veining and stockwork mineralization are typically associated with quartz-sericite alteration (cf. Figure 5a). Potassic alteration is most distinct at the Vesenny III and Nakhodka porphyry Cu-Au deposits. It typically consists of a reddish-brown fine-grained rock, which is locally overprinted by patchy quartz-sericite alteration assemblages. Relicts of primary magmatic biotite are

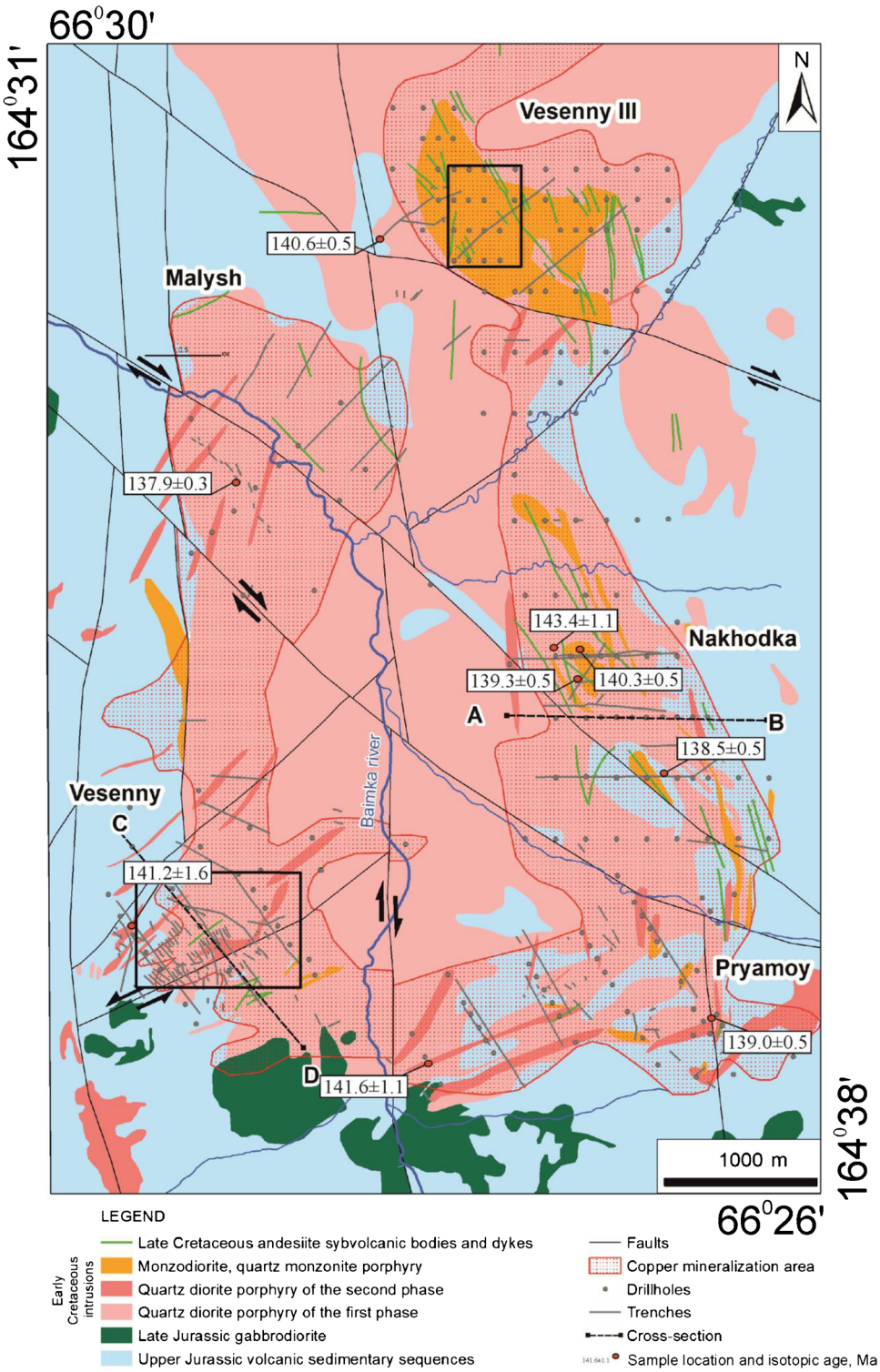

Fig. 4 Geological sketch map of the Nakhodka ore field, modified after Chitalin (2019a, b). The rectangles show the areas in Figs. 8 and 10

preserved in places but commonly replaced by magnesio-hastingsite and diopside phases and associated with abundant primary magnetite, the latter reflecting the high oxidation state of the igneous rocks. Biotite phenocrysts in fresh intrusions are dark brown and are defined by high TiO_2 concentrations of up to 5.19 wt% and $Fe_{tot}/(Fe_{tot} + Mg)$ ratios ranging between 0.30 and 0.35. By contrast, greenish hydrothermal biotite has much lower TiO_2 contents of < 0.95 wt% and lower $Fe_{tot}/(Fe_{tot} + Mg)$ ratios of 0.22–0.26, respectively.

The propylitic alteration assemblage forms a distinct aureole around the potassic and quartz-sericite core

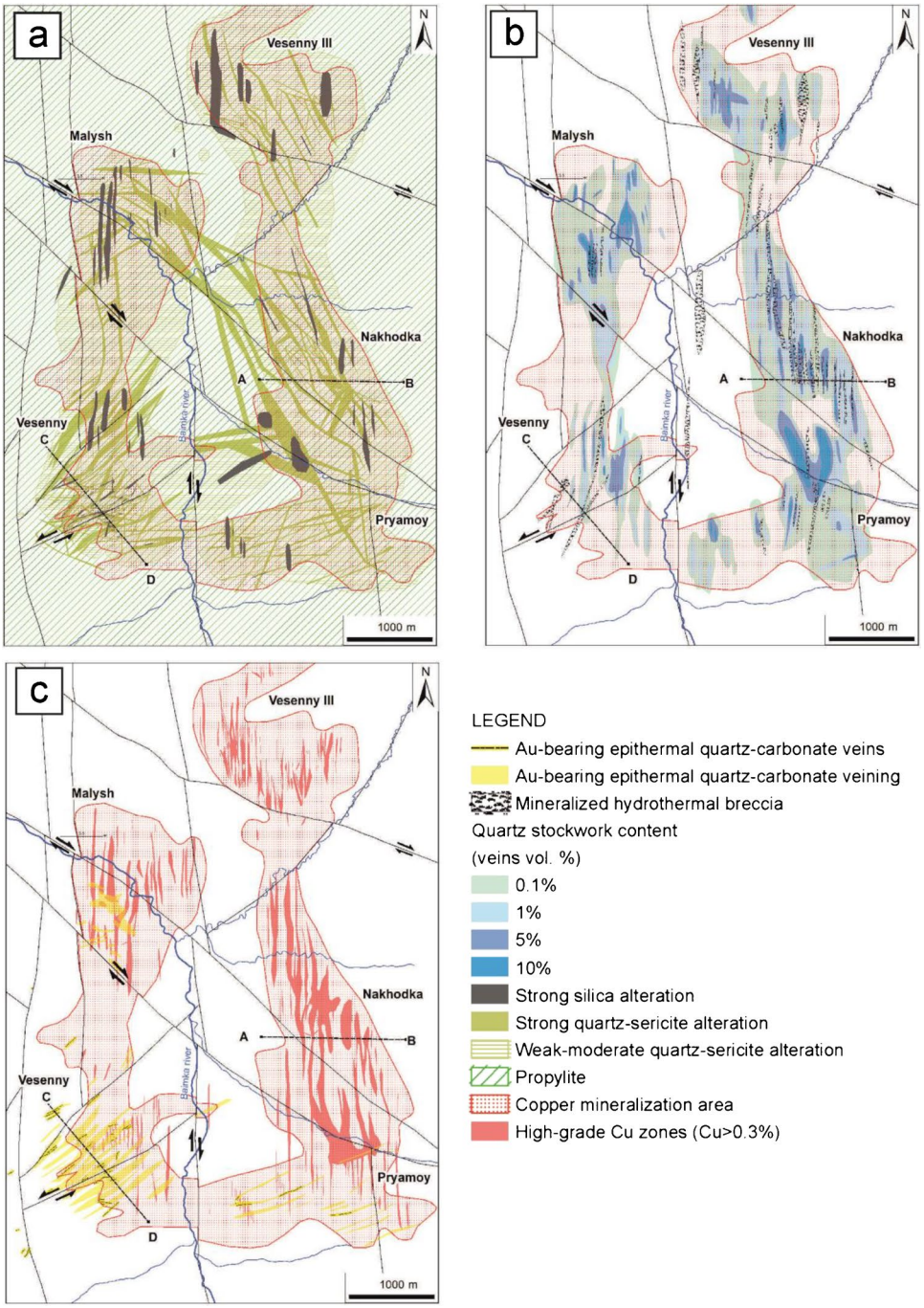

Fig. 5 Alteration and mineralization maps of the Nakhodka ore field, modified after Chitalin (2019a, b): **a** propylitic and quartz-sericite assemblages as well as pervasive silicification; **b** quartz-sulfide stockwork veining and hydrothermal breccias; **c** porphyry-style and epithermal-style gold mineralization

of the Nakhodka porphyry Cu-Au deposit, locally up to 1 km wide. The propylitic alteration overprints all igneous and volcano-sedimentary wall rock units and consists of earlier epidote and magnesio-hornblende and later actinolite, chlorite, quartz, albite and calcite. Primary magmatic magnesio-hastingsite and pyroxene phenocrysts are replaced by hydrothermal epidote and magnesio-hornblende; in turn, later actinolite, chlorite and calcite replace both earlier metasomatic and primary magmatic minerals. Clinochlore is the predominant chlorite phase.

The quartz-sericite alteration assemblage comprises hydrothermal sericite, quartz and pyrite and it includes local zones with patchy pervasive silicification and quartz-pyrite veining. In addition, sericite-altered rocks locally contain relict magnetite and zircon. Sericite can be mineralogically defined as muscovite and phengite. At Nakhodka, the porphyry Cu-Au mineralization and

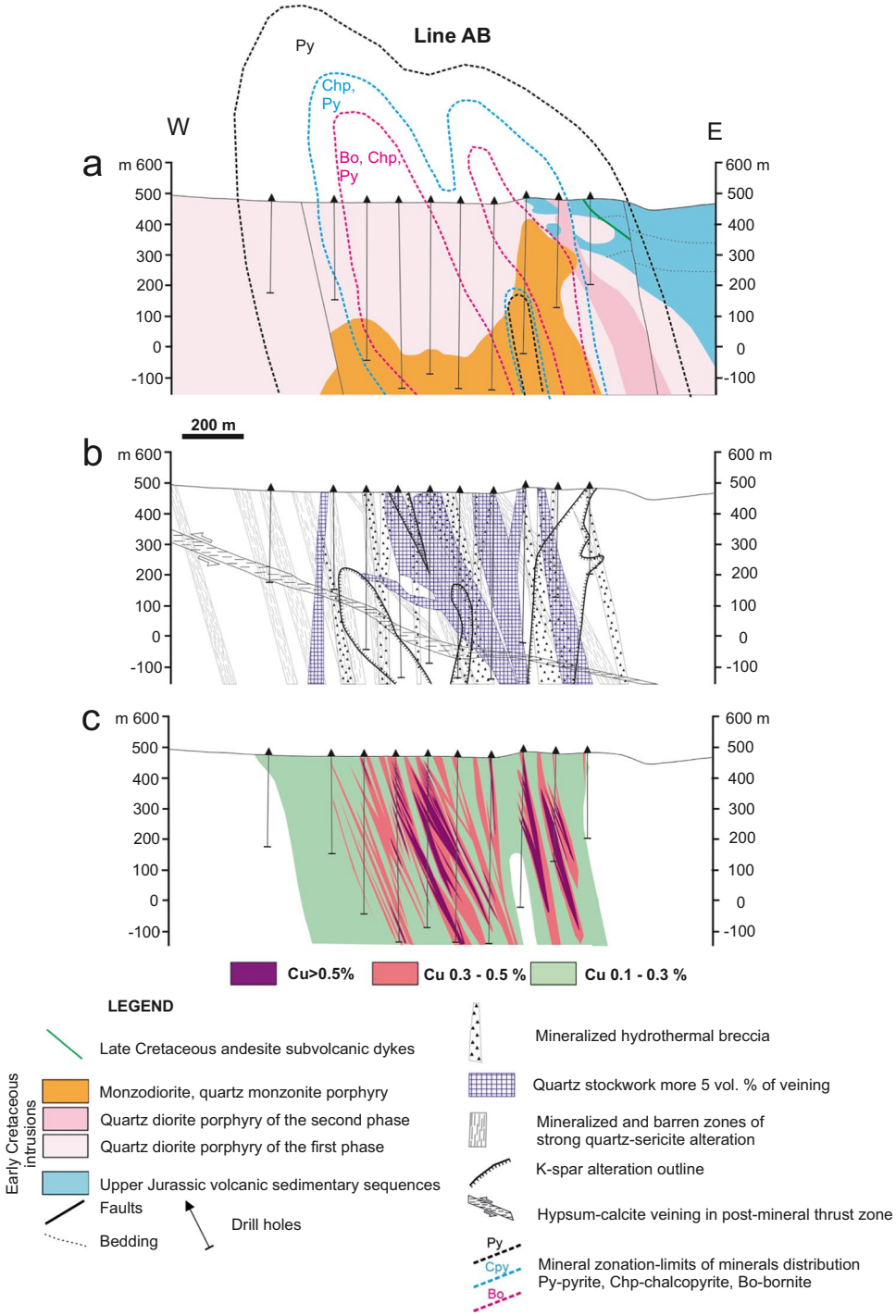

Fig. 6 Cross-sections across the Nakhodka deposit. Location of section line AB is shown in Fig. 5. Propylitic and weak quartz-sericite alteration zones are not shown (see Fig. 5a)

sheeted quartz-sulfide veining are generally associated with quartz-sericite alteration assemblages (Figs. 5b and 6). Their spatial distribution is typically structurally controlled by faults and fractures that also control the sheeted veining mineralization. Structurally controlled quartz-sericite zones vary in width between several mm and up to 20 m (ESM 2), extending along strike for tens or, locally, even hundreds of meters. These structures include NE- and NW-trending strike-slips as well as N-S and W-E oriented faults (Fig. 5a). In the central part of Nakhodka, there are several hydrothermal breccias with strong quartz-sericite alteration. The breccias consist of

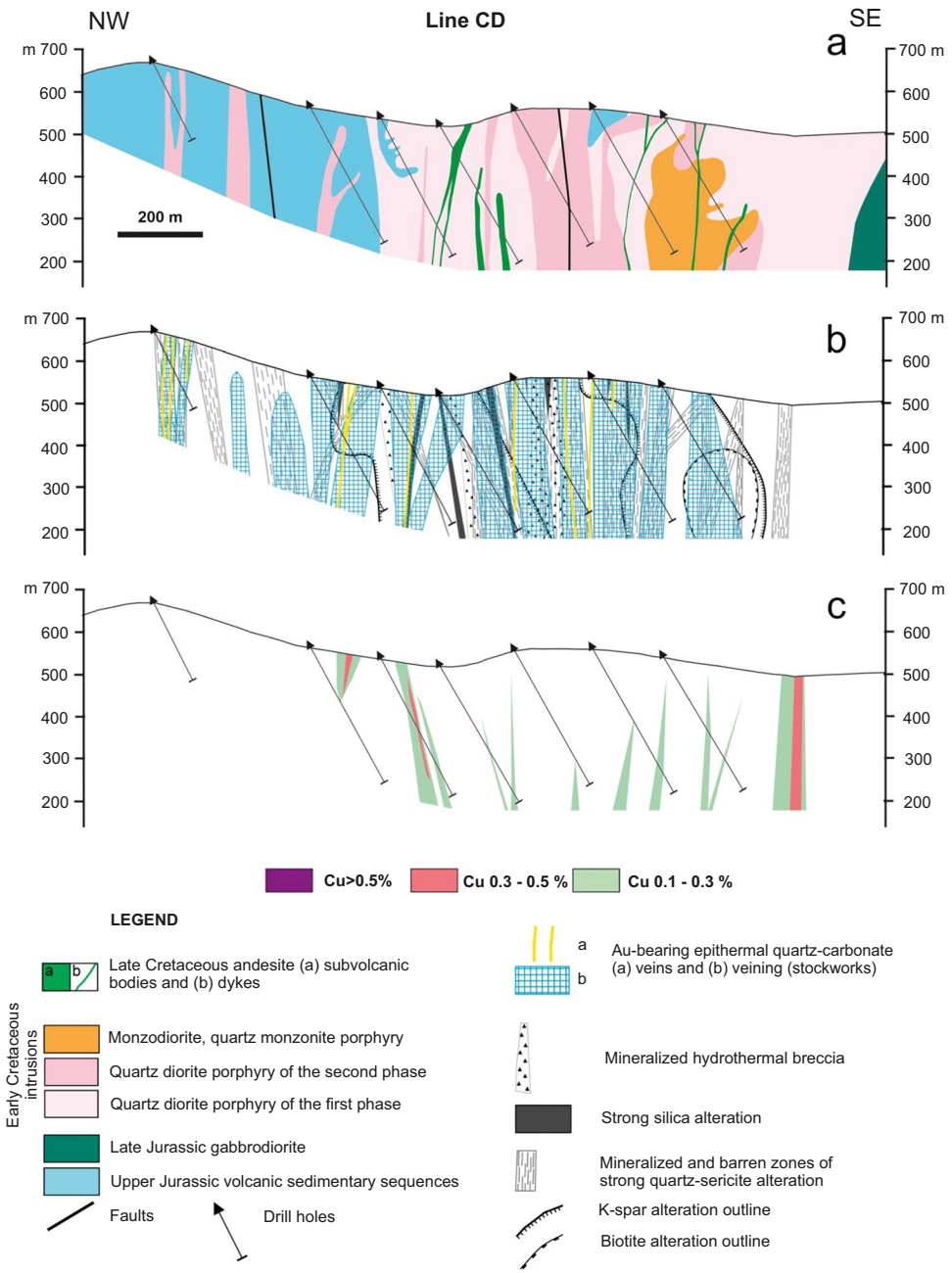

Fig. 7 Cross-sections across the Vesenny deposit. Location of section line CD is shown in Fig. 5. Propylitic and weak quartz-sericite alteration zones are not shown (see Fig. 5a): **a** geological section, **b** distribution of alteration styles and Au-bearing quartz-carbonate veins and stockworks, **c** distribution of copper grades

subangular clasts of quartz-sericite altered intrusions that are cemented by hydrothermal clays (ESM 2c, e, and f). In places, the hydrothermal breccias also contain large euhedral pyrite cubes measuring up to 1–2 cm in size.

Argillic alteration is only recorded in narrow zones measuring a few meters across. These argillic zones are mainly documented in the eastern part of the Pryamoy deposits (ESM 11). The drillhole samples of argillic alteration reveal a clay-dominated paragenesis comprising illite, dickite, high-Si clinochlore, quartz, and low-Fe dravite (Fig. 5c). Importantly, advanced argillic alteration is absent at Nakhodka, similar to the Peschanka porphyry Cu-Au deposit (Chitalin et al. 2021).

Importantly, all alteration assemblages at Nakhodka are post-dated and cross-cut by late-stage anhydrite-carbonate-quartz veining ranging from a few mm to 3 cm in width. Abundant late-stage anhydrite veins are also recorded at the nearby Peschanka porphyry Cu-Au deposit (Chitalin et al. 2021).

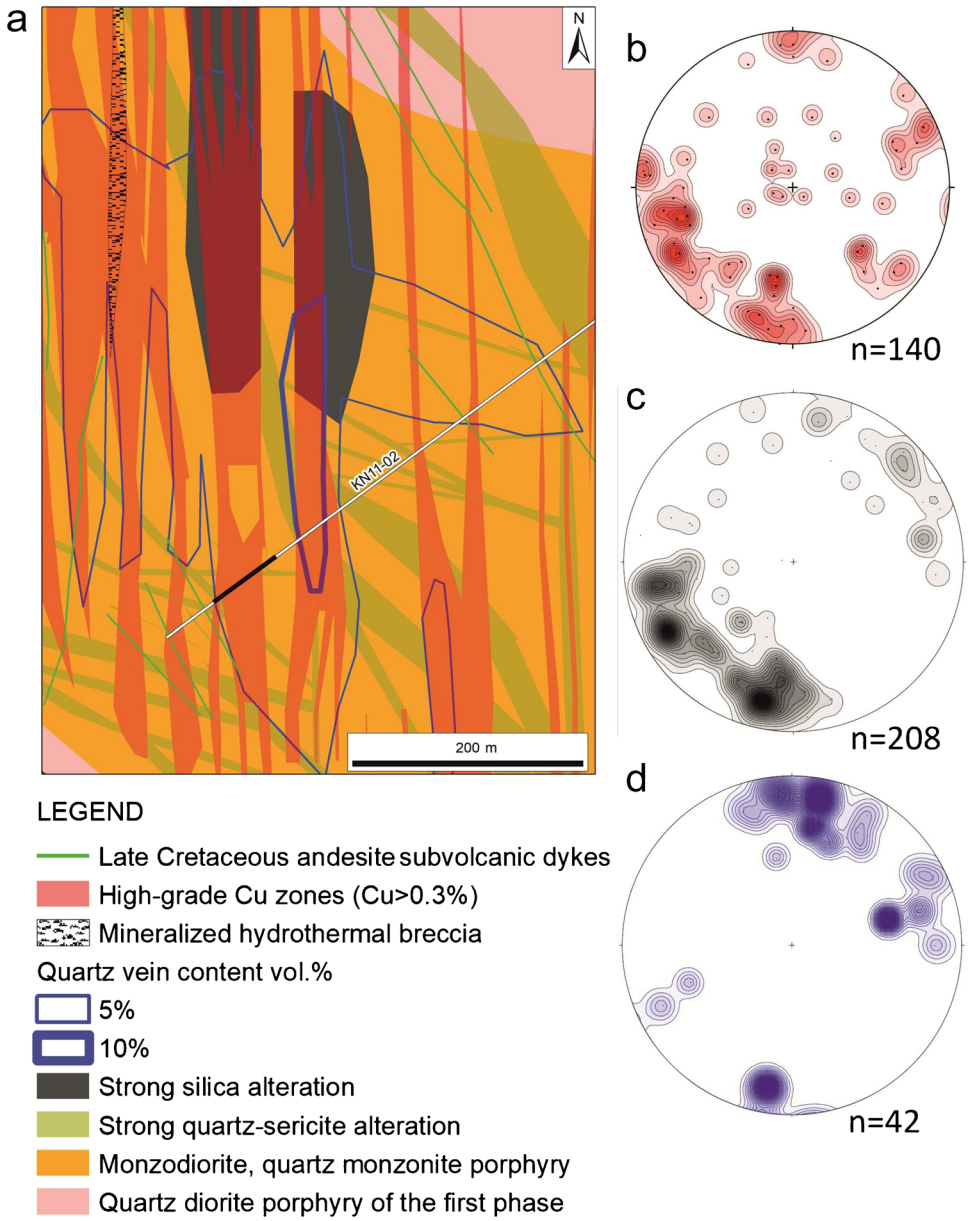

Fig. 8 Mineralized structures in the central part of the Vesenny III deposit. **a** Geological sketch map, see Fig. 4 for location. Black line shows the studied interval in the KN11-02 trench shown in ESM 7a. **b–d** Pole-to-plane stereograms for structures measured in the KN11-02 trench: **b** fractures, **c** quartz-sericite zones, **d** quartz veins. Lower hemisphere, contour intervals 1% per 1% area; *n* = number of structural planes

Mineralization in the Nakhodka ore field

The NOF represents a cluster of porphyry Cu-Au-Mo deposits that are locally overprinted and telescoped by intermediate-sulfidation epithermal Au–Ag veining. Both mineralization styles are described separately.

Porphyry Cu-Au stage

Three phases of porphyry-style mineralization are distinguished: (1) early-stage quartz-magnetite, magnetite ± chalcopyrite, and hematite veinlets and veins spatially associated with potassic alteration (ESM 3m); (2) sheeted quartz-sulfides (bornite, chalcopyrite, molybdenite, pyrite) veining with disseminated sulfides and spatially associated with quartz-sericite alteration assemblages (ESM 3k); and (3) mineralized hydrothermal breccia.

Sulfides, including bornite, chalcopyrite, pyrite, and molybdenite, are commonly disseminated in grey-glassy quartz veinlets or occur as fine bands along vein margins. Locally, sulfides are also documented along microfractures and in hydrothermal microbreccias (ESM 3d-l). The vein thickness ranges from 1 to 20 mm. Small near-vertical sheeted veining zones are less frequent. The sheeted veining mineralization is interpreted as the product of near horizontal extensional tectonics permitting mineralized hydrothermal fluids to percolate and precipitate their metal content during solidification (Chitalin et al. 2016). Pre-sulfide magnetite ± hematite ± quartz veins associated with potassic alteration (ESM 3m) are common at the Vesenny III and

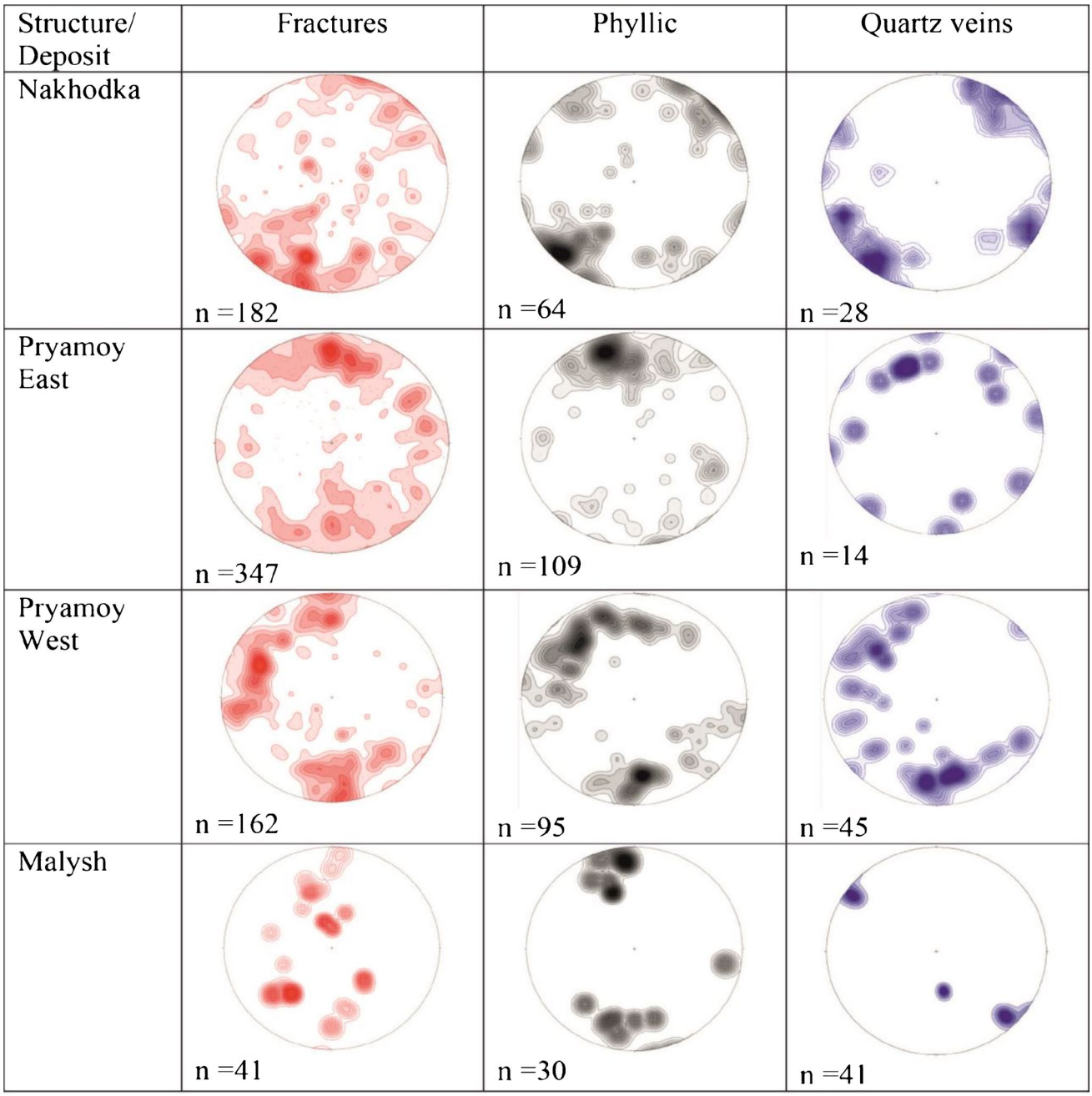

Fig. 9 Pole-to-plane stereograms for structures measured in the trenches at the Nakhodka, Pryamoy, and Malysh deposits. Lower hemisphere, contour intervals 1% per 1% area; *n* = number of structural planes

Nakhodka porphyry Cu-Au deposits. Post-mineral calcite, quartz, gypsum, anhydrite, and fluorite veinlets cut all rock units and quartz-sulfide veinlets of porphyry Cu-Mo stockworks (ESM 3n-o). The early-stage porphyry Cu-Au ± Mo mineralization in the NOF is clearly structurally controlled by NW- and NE-trending extensional strike-slip structures that acted as conduits for the hydrothermal fluids.

Hydrothermal breccias form N-S-trending elongated and near-vertical tabular bodies (Figs. 5b, 6, and 7). They post-date and cross-cut the porphyry-style mineralization. The size of the hydrothermal breccias ranges from a few centimetres to hundreds of meters, including individual breccia bodies of up to 150 m wide and up to 1500 m in length. Commonly, the hydrothermal breccias are irregular-shaped varying from small breccia veins to massive linear bodies with more or less tabular shapes, but locally splitting into several branches. The cement of the hydrothermal breccias is variable, including magnetite, hematite, quartz, pyrite,

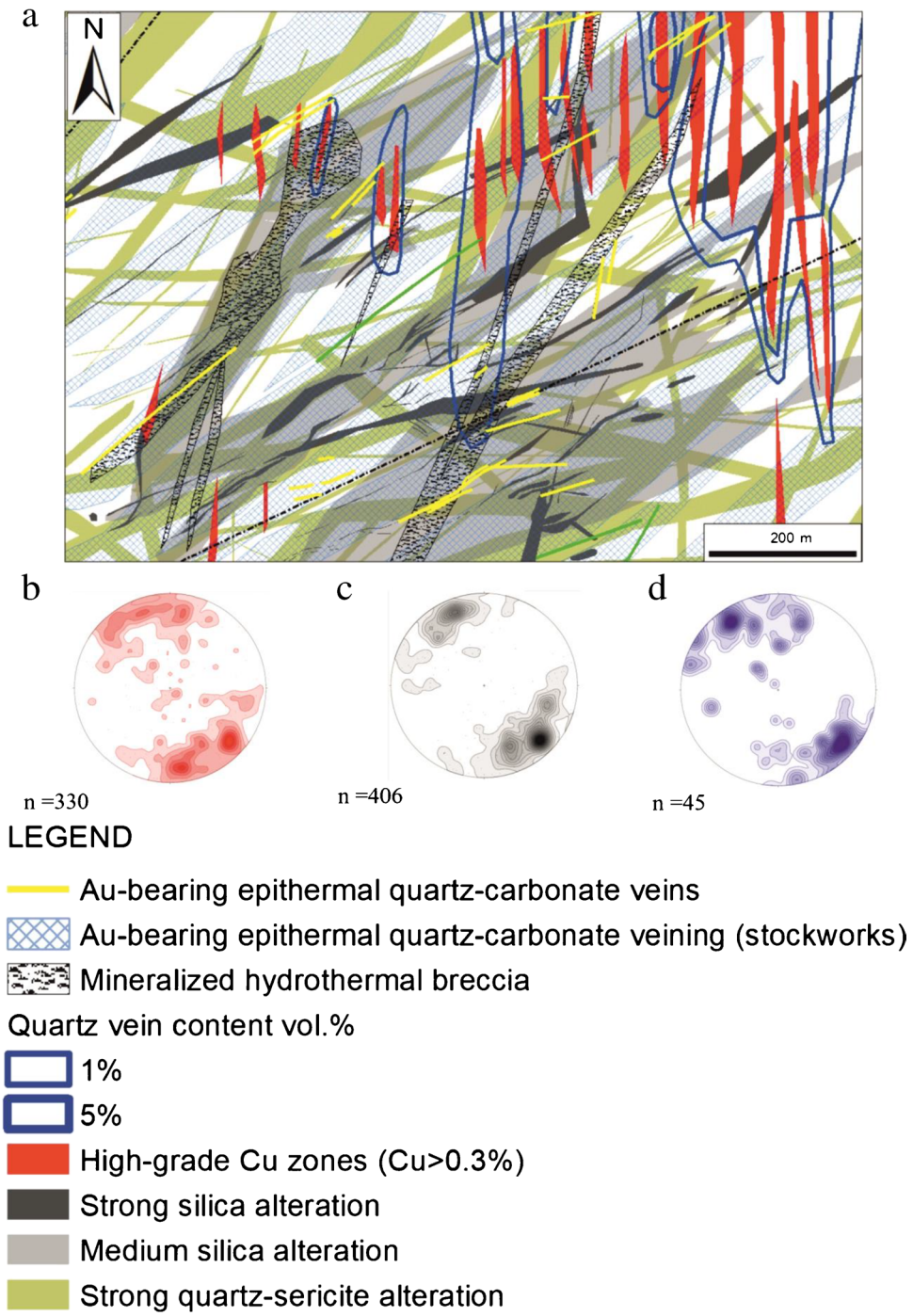

Fig. 10 **a** Alteration and mineralization map of the central part of the Vesenny deposit, modified after Chitalin (2016). See Fig. 4 for location. **b**–**d** Pole-to-plane stereograms for the structures measured in trenches: **b** Fractures, **c** Quartz-sericite zones, and quartz-carbonate veins. Lower hemisphere, contour intervals 1% per 1% area; *n* = number of structural planes

chalcopyrite, pyrite, and locally fluorite. The fragments of the breccias may be angular, sub-angular, or sub-rounded, respectively (ESM 4).

Bornite is most abundant at the Vesenny III and the Nakhodka deposits and, to a lesser amount, also at the Pryamoy deposit. At the Vesenny deposit, bornite is less common, but it is recorded in deep drill intersections. At the Malysh deposit, bornite is restricted to minor inclusions in pyrite crystals. At Nakhodka, bornite phases can measure up to several mm in size, commonly with chalcopyrite exsolution lamellae (ESM 12a and b; see also: Nagornaya 2013). In places, bornite contains inclusions of native gold with a distinctly high fineness (917–926), clausthalite, Se-rich galena, altaite, and tetradymite. Bornite phases may also contain elevated Ag contents of up to 0.33 wt%.

Chalcopyrite either forms exsolution lamellae in bornite or it occurs as overgrowths and replacements of bornite (ESM 12a, c; see also: Nagornaya 2013); also, it is

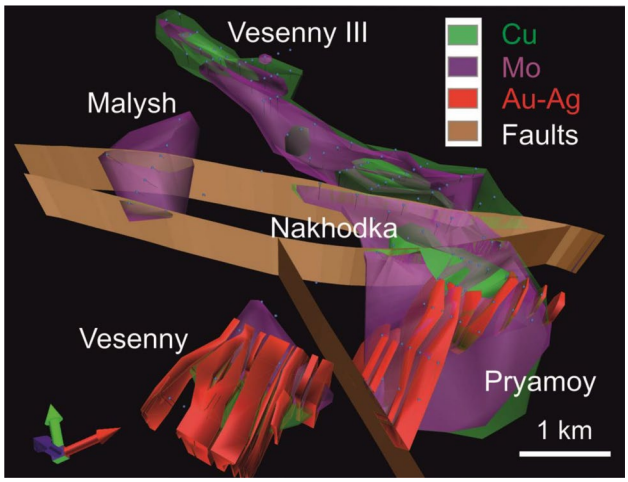

Fig. 11 3D model of mineralized stockworks at the Nakhodka ore field (modified after Chitalin et al. 2016, 2020). Copper and Mo mark porphyry Cu and Mo stockworks, while Ag–Ag mark epithermal stockworks and veins, respectively

intergrown with molybdenite and occurs as inclusions in pyrite (ESM 12e, f). The size of chalcopyrite grains can be up to 3 mm across. In the oxidation zone, chalcopyrite is partly replaced by covellite or brochantite as well as Cu-bearing aluminites (Nagornaya 2013).

Molybdenite is abundant at the Malysh porphyry deposit, but rare at the other deposits of the Nakhodka ore field. It typically forms fine flakes up to a few hundred micrometers across. Locally, these flakes can form clusters ranging up to a few mm in size or they occur as fracture fill, particularly in quartz-sericite altered rocks (ESM 12d, e; see also: Nagornaya 2013). ICP-MS studies by Nagornaya (2013) reveal high, but variable, Re content in molybdenite ranging between 21 and 1439 ppm. In the oxidation zone, molybdenite is commonly replaced by ferrimolybdite.

Pyrite typically occurs as euhedral grains ranging in size from a few micrometers to several mm. Importantly, the pyrite crystals are unzoned (ESM 12f; see also: Nagornaya 2013). In the oxidation zone, pyrite is replaced by limonite.

Epithermal stage

Intermediate-sulfidation epithermal gold-bearing polymetallic quartz-dolomite ± rhodochrosite veins and veinlets (ESM 5a, b) are mainly documented at the Malysh, Vesenny, and Pryamoy deposits (ESM 5c, e). They overprint and locally intersect the early-stage porphyry-style mineralization and related hydrothermal breccias. Arsenian pyrite, galena, sphalerite, chalcopyrite, and sulfosalts are the main epithermal ore minerals at Nakhodka. Minor constituents are Au–Ag alloys, hessite, altaite and clausthalite, with rare petzite, enargite, pearceite, acanthite, and various Se- and Te-bearing minerals, respectively. The epithermal overprint appears to be geochemically zoned (Fig. 4) with Te-rich sulfides and tellurides most common in the southern part of the NOF (e.g., Vesenny and Pryamoy deposits) and Se-rich minerals and selenides mainly documented in the northern part (e.g., Malysh deposit). Epithermal quartz-carbonate ± rhodochrosite veins (ESM 5a, b) and veinlet stockworks (ESM 5e) are documented at the Malysh, Vesenny, and Pryamoy deposits. They overprint and intersect the early-stage porphyry-style mineralization and hydrothermal breccias (ESM 5c, d). Epithermal veining is intersected by exploration drilling to depths of up to 450 m (Chitalin et al. 2013, 2016).

Pyrite forms euhedral crystals of up to 5 mm in size, in places, containing small chalcopyrite inclusions. The epithermal pyrite phases are zoned and contain high As contents up to 10.5 wt% (ESM 13a; see also: Nagornaya 2013). During the evolution of the hydrothermal system, the As-rich zones of the pyrite were partly corroded and thus representing a possible source for the high As content of late-stage sulfosalts. Pyrite grains at the Malysh deposit may contain inclusions of native tellurium, hessite, and Se-rich galena (ESM 13f, g, h). Unfortunately, the very small size of most inclusions prevents their detailed documentation by quantitative electron microprobe analysis.

Chalcopyrite is rare in the epithermal assemblage. Chalcopyrite phases from this stage are commonly rimmed by enargite and closely associated with Cu-rich tennantite and sphalerite, either forming disseminations or occurring in stringer veins. At the Malysh deposit, epithermal chalcopyrite phases may contain inclusions of Se-rich galena and clausthalite (ESM 13).

Sphalerite occurs as the brown, Fe-rich variety typically > 500 µm across and as the honey brown, Cd-rich variety ranging in size from the micrometer scale to up to 5 mm. The first variety has relatively high Fe content of up to 11.8 wt% and it contains up to 6.5 wt% Cu. By contrast, the second sphalerite variety has much lower Fe and Cu concentrations of < 4.6 and < 2.4 wt%, respectively. Sphalerite of both types is locally replaced by sulfosalts.

Galena either forms isolated grains of variable size or crystal aggregates. In places, it is intergrown with sphalerite and sulfosalts. Galena also occurs as fracture filling in arsenian pyrite, chalcopyrite, and sphalerite phases.

Enargite occurs as rims around chalcopyrite phases or as individual phases measuring up to 100 µm in size, commonly associated with Cu-rich tennantite (ESM 13c, d; see also: Nagornaya 2013). Although enargite is considered as a typical mineral for the high-sulfidation epithermal environment, there is a distinct lack of any advanced argillic alteration in the Nakhodka ore field.

Sulfosalts from the Nakhodka ore field are documented in detail by Marushchenko et al. (2018). Hence, we only briefly

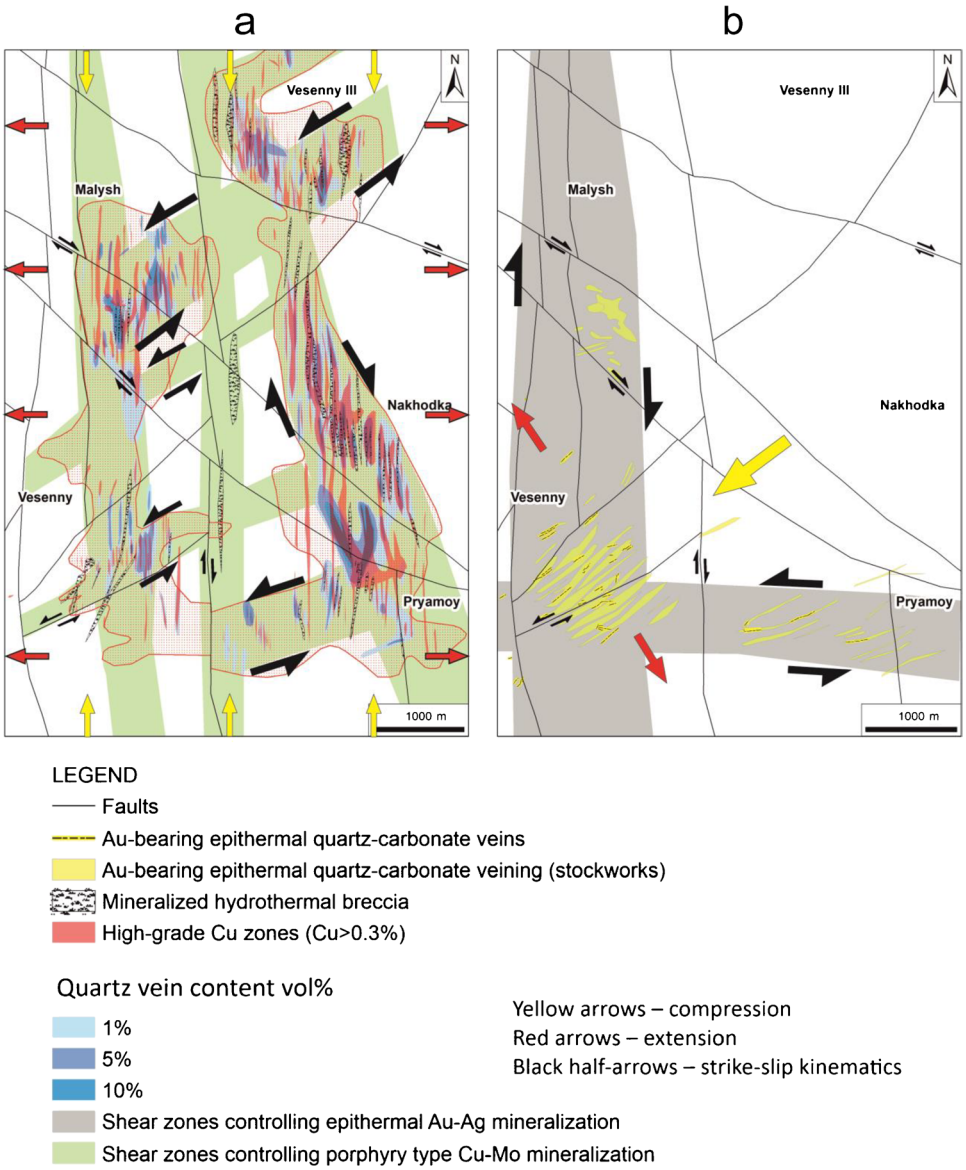

Fig. 12 Structural models of the Nakhodka ore field stockworks, modified after Chitalin (2021): **a** porphyry Cu-Mo-Au stockwork zones; **b** epithermal Au–Ag stockwork zones

describe their mineralogy. The documented sulfosalts typically measure < 50 µm in size, and they either form inclusions in zoned arsenian pyrite, fracture fills in chalcopyrite, or partial replacements of sphalerite. Silver-rich (2.6–4.1 wt%) tetrahedrite is recorded at the Vesenny deposit. Tennantite is mainly recorded in the central part of the NOF, while Ag-rich tetrahedrite is observed in the northern and southern parts, respectively (Nagornaya 2013).

Gold-silver alloys are documented by Nikolaev et al. (2016). The grains range from 2 to 30 µm in size and form microinclusions in pyrite, galena, and sulfosalts, commonly intergrown with hessite and petzite. Individual gold alloy grains are weakly zoned, and are normally with Ag-rich rim. The gold fineness is variable and ranges between 857 and 657. Detailed mineralogical studies by Nikolaev et al. (2016) reveal that hessite, petzite, stützite, pearceite, and acanthite represent the main silver minerals at the Vesenny and Pryamoy deposits.

Post-mineral calcite, gypsum, and anhydrite veinlets are common. Supergene mineralization in the oxidation zone comprises copper carbonates and sulfates, copper wad, and minor covellite. Chalcocite is very rare. Importantly, there is a distinct lack of advanced argillic alteration assemblages, similar to the Peschanka porphyry Cu-Au ± Mo deposit (Chitalin et al. 2021).

Zonation based on bulk-rock geochemistry

The zonation of the NOF derived from the bulk-rock geochemistry is described in detail by Khabibullina (nee Sidorina 2015) and summarized below.

Six dominant element associations, which spatially correlate with the mineralogical assemblages of the main ore stages, were identified by factor analysis and illustrate the lateral geochemical zoning of the NOF (ESM 14a).

The Fe–Mn-Au association forms the outer horseshoe-shaped shell around the ore field. The Mo-Cu association represents the chalcopyrite-molybdenite assemblage of the porphyry Cu-Mo stockwork mineralization in the center. The stockwork bornite zones are represented by the Cu-Bi-Se association. The inner part of the horseshoe structure is barren.

The Sb-As-Cu-Se association corresponds to the tetrahedrite-group minerals post-dating and superimposing all other geochemical associations. The Zn-Pb–Cd-Mn-Ag-Au and Te-Au-Se-Ag associations show similar distribution. Geochemically, these types represent the IS epithermal mineralization.

The distribution of the elements and their respective ratios along our cross sections suggest that the Ag + Pb + Zn/Cu + Bi + Mo ratio could be used as a proxy for the erosion level of the system during epithermal mineralization stage (ESM 14b). However, no any significant vertical movements, which could result in different erosion level of the NOF deposits, are observed. Therefore, this ratio may be a proxy of development degree of epithermal mineralization, rather than erosion level. The numerator represents the key elements of the epithermal stage post-dating and overprinting the porphyry mineralization. The major elements of the porphyry stage form the denominator, respectively. The average metal grades at a definite elevation were used for the calculation of the Ag + Pb + Zn/Cu + Bi + Mo value. The development degree of the epithermal system in the NOF gradually decreases as follows: Vesenny → Pryamoy → Nakhodka → Vesenny III.

Geochemical composition of the Nakhodka host intrusions

According to Volchkov et al. (1982) and Soloviev (2014), the Nakhodka monzodiorite-monzonite intrusions are defined by high whole-rock K_2O contents of up to 4.57 wt% and high K_2O/Na_2O ratios ranging between 0.7 and 0.9, respectively. However, those initial whole-rock geochemical studies only include major oxide concentrations and thus our study provides the first high-precision trace-element data from the Nakhodka intrusions (ESM 15). Unfortunately, during recent exploration programs, only trace-element geochemistry was obtained from the Nakhodka intrusions.

Importantly, the monzodiorites are defined by high LILE contents (e.g., Sr of up to 1089 ppm and Ba of up to 5823 ppm) and elevated LREE (e.g., La of up to 23 and Ce of up to 48 ppm), respectively (ESM 15). Their high LILE and LREE, as well as diagnostically low HFSE concentrations (Hf < 1.85 ppm, Nb < 3.5 ppm, Y < 18 ppm and Zr < 58 ppm) reveal a paleo-island arc setting of the NOF, a similar tectonic setting as the Peschanka porphyry Cu-Au deposit in the vicinity (Chitalin et al. 2021). A paleo-subduction setting is also implied by plotting the samples on the Nb versus Y discrimination diagram (ESM 16a).

The Nakhodka intrusions are also defined by high whole-rock La/Yb ratios of up to 16.7, and high Ta/Yb and Th/Yb ratios of up to 0.58 and 3.75, respectively, reflecting their high-K calc-alkaline compositions (cf. ESM 16c). Trace elements such as Ta, Th, and La are considered to behave immobile even during hydrothermal alteration (Pearce 1982; Müller et al. 1992). ESM 16 also illustrates that the Nakhodka intrusions have slightly lower Nb contents of < 3.5 ppm and whole-rock Th/Yb ratios of < 3.7 when compared to those from Peschanka (Chitalin et al. 2021).

Importantly, the whole-rock Eu/Eu* ratios of the Nakhodka intrusions are > 1, which is common for intrusions with high oxidation state (Loader et al. 2017). Abundant amphibole and biotite phenocrysts as well as high whole-rock Sr/Y ratios of up to 62.3 in the NOF intrusions reflect the distinctly high water contents of their parental melts (ESM 15).

Geophysical footprint of the Nakhodka ore field

Ground-magnetic surveys on the 1:20 000 scale were carried out in 2011 (Chitalin et al. 2014). The Nakhodka porphyry Cu-Au deposit and the Vesenny III and Pryamoy deposits are defined by distinct positive magnetic anomalies, but with different intensities. Importantly, these magnetic anomalies broadly overlap with significant IP chargeability and resistivity anomalies. ESM 17 illustrates a significant chargeability anomaly surrounding the entire NOF. Exploration drilling reveals that chargeability anomalies directly correlate with intense pyrite-rich quartz-sericite alteration, locally containing up to 10 vol% of disseminated pyrite. In places, there are linear high resistivity anomalies reflecting concealed faults and/or structurally controlled zones with strong silicification.

High-grade Cu-Au stockwork zones at the Vesenny III deposit as well as hydrothermal breccias are defined by very high magnetic anomalies caused by strong hydrothermal magnetite veining and breccias associated with biotite-magnetite alteration. However, as evident by the drill testing of these anomalies, the higher the copper content, the higher the hematite content. In other words, magnetite causing the high magnetic anomaly is of relic nature. By contrast, the stockwork mineralization at the Nakhodka and Pryamoy porphyry Cu-Au deposits is associated with strong quartz-sericite alteration assemblages with abundant hematite, the

latter likely replacing magnetite due to martitization, and resulting in low magnetic anomalies (ESM 17). In places, high magnetic anomalies are beyond outlined copper mineralization (ESM 17); all of them are associated with Jurassic sequences probably representing concealed gabbro or potassic altered monzonite intrusions. However, these local magnetic highs are not drill-tested. At the same time, the copper outline broader than the magnetic high supports our opinion that copper mineralization is not associated with the high magnetic potassic alteration.

An audi-magneto-telluric survey reveals extensive low-resistivity anomalies reflecting concealed veining and stockwork mineralization both at the Nakhodka and Vesenny deposits and down to vertical depths of at least 600 and 1000 m, respectively, as documented by deep exploration drilling.

Exploration drilling also confirms the vertical extensions of significant chalcopyrite-bornite-molybdenite mineralization down to vertical depths of at least 600 m at Nakhodka and open at depth.

The Vesenny epithermal Au–Ag deposit is defined by a strong negative magnetic anomaly caused by both strong silicification and magnetite-destructive quartz-sericite to argillic alteration of the parental diorite intrusions in conjunction with significant quartz-carbonate veining.

Discussion

Recent studies suggest that a favorable structural setting represents a key factor in the formation of world-class porphyry Cu-Au deposits (e.g., Groves et al. 2022). Porphyry Cu-Au clusters are commonly located near the intersections between arc-parallel crustal-scale faults and high-angle oblique transform or accommodation faults (Corbett and Leach 1998; Matteini et al. 2002; Gow and Walshe 2005). Nakhodka is a structurally controlled porphyry Cu-Au deposit and the prevailing stress field during its evolution has led to the formation of extensional and dextral strike-slip faults controlling high-grade sheeted quartz–bornite veining. The structural setting of Nakhodka is similar to the Peschanka porphyry Cu-Au deposit located about 20 km to the NW (Chitalin et al. 2022). All documented large porphyry Cu-Au deposits and associated occurrences are situated in the Baimka structural (strike-slip) trend. Favorable structural trends also control the location of other world-class porphyry Cu-Au deposits such as Oyu Tolgoi, Mongolia and Pebble, Alaska (Kirwin et al. 2005; Ghaffari et al. 2011; Olson et al., 2017; AMC Consultants Pty 2020) or Chuquicamata, Chile (Ossandón et al. 2001). Oyu Tolgoi represents a cluster of six porphyry Cu-Au systems following a linear NE trend of the underlying magma chamber (Crane and Kavalieris 2012), comparable to the linear, but NW-oriented, Baimka Trend hosting the Peschanka and Nakhodka porphyry Cu-Au clusters in Siberia (Chitalin et al. 2022). The large pebble porphyry Cu-Au deposit in Alaska is controlled by NE-trending structures (Olson et al. 2017). Importantly, all of these world-class porphyry Cu-Au deposits share a similar tectonic setting comprising of an amalgamation of Cretaceous island arcs (Crane and Kavalieris 2012; Olson et al. 2017; Müller and Groves 2019).

In places, the early-stage porphyry Cu-Au deposits of the Nakhodka cluster are overprinted and telescoped by epithermal-style Au–Ag mineralization (e.g., at Vesenny and Pryamoy), probably due to tectonic uplift and denudation. Telescoping of epithermal mineralization on top of porphyry system is a common phenomenon in geological settings with significant tectonic uplift rates and denudation (Corbett and Leach 1998; Sillitoe and Hedenquist 2003). Well-documented examples are the Rosario porphyry Cu-Mo, Chile (Masterman et al. 2005) as well as the Altar (Maydagan et al. 2020) and Josemaria porphyry Cu deposits, Argentina (Sillitoe et al. 2019). Telescoped porphyry-epithermal Cu-Au systems are interpreted to reflect synmineral erosion, progressive paleosurface lowering and alteration-mineralization overlapping as a result of compressive deformation and uplift (Sillitoe et al. 2019; Maydagan et al. 2020).

The illite-quartz-dolomite-rhodochrosite alteration paragenesis at Nakhodka, especially at the Vesenny and Pryamoy deposits (Nagornaya 2013; Nagornaya et al. 2012; Marushchenko et al. 2018), is similar to the alteration assemblage of the Capillitas Cu prospect in the Catamarca Province of NW Argentina (Marquez-Zavalia and Heinrich 2016). Capillitas belongs to the Farallon Negro cluster of porphyry Cu-Au and epithermal Au systems including the world-class Bajo de la Alumbrera porphyry Cu-Au deposit as well as the Agua Rica porphyry Cu-Au and Cerro Atajo and Cerro Durazno epithermal Au prospects (Müller and Forrestal 1998; Von Quadt et al. 2011; Franchini et al. 2011, 2015; Marquez-Zavalia and Heinrich 2016). Importantly, in both mineral districts, Nakhodka and Farallon Negro, the epithermal Au and porphyry Au-Cu mineralization is hosted by high-K intrusions (cf. Landtwing 1998; Müller and Forrestal 1998).

High-grade sheeted quartz-bornite veining is commonly associated with strong quartz-sericite alteration at Nakhodka as well as at the Vesenny III, Praymoy, and Malysh porphyry Cu-Au deposits. We interpret this paragenesis as evidence for multiple, and overprinting, phases of porphyry-style mineralization, because quartz-sericite alteration typically forms at slightly lower temperatures than potassic assemblages at the core of the hydrothermal system. Similar to Peschanka, the NOF is characterized by a complete lack of advanced argillic alteration assemblages (cf. Chitalin et al. 2022), possibly due to erosion. However, there is no evidence for

the diagostic actinolite-albite (i.e., sodic-calcic) alteration assemblages, neither on surface nor in deep intercepts, suggesting a relatively high preservation level of Nakhodka.

The Nakhodka, Vesenny III, and Pryamoy deposits are defined by distinct positive magnetic anomalies which broadly overlap with significant IP chargeability and resistivity anomalies. High-grade Cu-Au stockwork zones at the Vesenny III deposit as well as hydrothermal breccias are defined by strong magnetic anomalies due to hydrothermal magnetite veining and breccias associated with potassic alteration. By contrast, the stockwork mineralization at the Nakhodka and Pryamoy porphyry Cu-Au deposits are locally overprinted by strong quartz-sericite alteration assemblages resulting in magnetite destruction (cf. Kwan and Müller 2020).

The gold-rich Nakhodka porphyry Cu system is hosted by, with decreasing intrusion ages, porphyritic diorite, monzodiorite, and monzonite phases. Monzodiorites and monzonites have high-K calc-alkaline compositions and host numerous world-class porphyry Au or porphyry Cu-Au deposits such as Grasberg, Indonesia (Pollard et al. 2005); Kişladağ, Turkey (Baker et al. 2016); Ok Tedi, Papua New Guinea (Large et al. 2018); Oyu Tolgoi, Mongolia (Crane and Kavalieris 2012); Pebble, Alaska (Olson et al. 2017); and Reko Diq, Pakistan (Richards et al. 2018). Geochemically, the parental intrusions of the NOF are almost identical to those hosting the Peschanka porphyry Cu-Au deposit (Chitalin et al. 2022) in having distinctly low HFSE (e.g., Hf ≤ 1.69 ppm, Nb ≤ 3.55 ppm and Zr ≤ 58.8 ppm) and LREE contents (La ≤ 23.8 ppm and Ce ≤ 48.2 ppm), respectively, that are typical for igneous intrusions emplaced in island arc-settings (cf. Müller et al. 1992). These diagnostic geochemical fingerprints confirm previous geological interpretations by Parfenov (1991) and Nokleberg et al. (2000). However, the Nakhodka intrusions have slightly lower Nb contents than those at Peschanka resulting in lower Nb/Y ratios of < 0.8 (ESM 1 and ESM 16). Importantly, their whole-rock Th/Yb and Ta/Yb ratios are almost indistinguishable from those of the Peschanka intrusions and record their high-K calc-alkaline composition (cf. Pearce 1982). Importantly, the Nakhodka intrusions are defined by both high oxidation state and high magmatic H_2O content. The high whole-rock Eu/Eu* ratios of the Nakhodka intrusions of 1.03–1.97 and very high V/Sc ratios of up to 97 are interpreted as proxies for their high oxidation state. High magmatic water content of the Nakhodka intrusions is documented by abundant amphibole phenocrysts and high whole-rock Sr/Y ratios of up to 62.3 (cf. Richards 2011) and may be compared to the parental intrusions at other world-class porphyry Cu-Au deposits worldwide (Müller and Groves 2019, and references therein).

Conclusions

The Nakhodka ore field represents a cluster of porphyry Au-Cu and IS epithermal Au–Ag deposits in the Baimka Trend, NE Siberia, Russia. Porphyry Cu-Au ± Mo and Au–Ag mineralization is hosted by H_2O-rich composite diorite, monzodiorite and monzonite porphyry intrusions with distinctly high oxidation state. These parental stocks have high-K calc-alkaline composition and are dated at about 139–141 Ma based on U–Pb zircon ages. The geological framework and the whole-rock trace-element compositions of these intrusions with diagnostically low HFSE contents reveal that the parental stocks were emplaced in a tectonic amalgamation of paleo-island arcs.

The Nakhodka intrusions are overprinted by widespread hydrothermal alteration including potassic, propylitic and quartz-sericite assemblages as well as local zones of silicification. By contrast, argillic alteration zones are rare and advanced argillic alteration assemblages are lacking. Locally, the porphyry-style Cu-Au-Mo mineralization is overprinted by late-stage intermediate-sulfidation epithermal Au–Ag veins.

Porphyry-style mineralization at Nakhodka is clearly structurally controlled and the N-S orientation of the porphyry-related veins and high-grade sheeted veining zones is controlled by extensional structures, similar to the giant Peschanka porphyry Cu-Au-Mo deposit in the vicinity. Additionally, the epithermal vein systems in the NOF are controlled by extensional en-echelon structures within conjugate shear zones.

Based on the geochemical zonation, the development degree of epithermal mineralization decreases from the Vesenny deposit in the south through Pryamoy and Nakhodka to the Vesenny III deposit in the northern part. The world-class Nakhodka porphyry Cu-Au deposit and the Vesenny III and Pryamoy deposits are defined by distinct positive magnetic anomalies which broadly overlap with significant IP chargeability and resistivity anomalies.

Supplementary Information The online version contains supplementary material available at https://doi.org/10.1007/s00126-022-01122-2.

Acknowledgements We would like to sincerely thank Bernd Lehmann, Reimar Seltmann, and Andreas Dietrich for reading the manuscript, for correcting it, and for their constructive comments and suggestions which resulted in greatly improving it.

Funding The results of section "Geochemical composition of the Nakhodka host intrusions" were obtained within the Russian Science Foundation grant (project no. 19–17-00200). The work by Ekaterina V. Nagornaya was supported by Federal budget (project no. 0137–2019-0012 "Petrology, geochemistry, and geodynamics of the formation and evolution of the oceanic and continental lithospheres").

Declarations

Conflict of Interest The authors declare no competing interests.

References

Akinin VV, Miller EL (2011) Evolution of calc-alkaline magmas of the Okhotsk-Chukotka volcanic belt. Petrology 19:237–277. https://doi.org/10.1134/s0869591111020020

AMC Consultants Pty. Ltd. (2020) Oyu Tolgoi 2020 technical report. https://turquoisehill.com/turquoise-hill/technical-reports/default.aspx. Accessed 15 November 2021

Baker T, Bickford D, Juras S, Lewis P, Oztas Y, Ross K, Tukac A, Rabayrol F, Miskovic A, Friedman R, Creaser RA, Spikings R (2016) The geology of the Kişladağ, porphyry gold deposit, Turkey. Econ Geol Spec Publ 19:57–84

Chitalin AF (2019a) Structural paragenesis and ore mineralization of the Baimskaya shear zone, Western Chukotka. In: Russian Tectonophysics. On the occasion of the 100th anniversary of M.V. Gzovsky. RIO KSC RAS, Apatity, pp. 333–349 [in Russian]

Chitalin AF (2019b) Geological-structural interpretation of geophysical and geochemical anomalies of the Baimskaya Ore Zone, Western Chukotka. Abstracts, International Geological-Geophysical Conference "GeoEurasia 2019b", Moscow, pp. 961–966 [in Russian]

Chitalin AF (2021) The structure of stockworks of Porphyry Copper systems. Abstracts "GeoEurasia 2021" International Geological and Geophysical Conference. pp 171–176 [in Russian]

Chitalin A, Fomichev E, Usenko V, Agapitov D, Shtengelov A (2012) Structural model of Peschanka porphyry Cu-Au-Mo deposit, Western Chukotka, Russia. Poster, Structural Geology and Resources-2012. https://igeotech.ru/wp-content/uploads/2020/04/a.-chitalin-structural-model-of-peschanka-porphyry-cu-au-mo_abstractproofs.pdf. Accessed 15 November 2021

Chitalin AF, Usenko VV, Fomichev EV (2013) The Baimka ore zone – a cluster of large base and precious metal deposits in the at the west of the Chukchi Autonomous Okrug. Mineral Resources of Russia: Economics and Management 6:68–73 [in Russian]

Chitalin AF, Nikolaev YuN, Shtengelov AR, Fomichev EV, Usenko VV, Shatnov VY, Baksheev IA, Sidorina YN, Djedjeya GT, Kalko IA, Apletalin AV, Okhapkina EY, Nagornaya EV, Marustchenko LI, Kuzkin AC (2014) Exploration work in Baimka licensed area. Unpubl Report [in Russian]

Chitalin AF, Nikolaev YuN, Baksheev IA, Prokofiev VYu, Fomichev EV, Usenko VV, Nagornay EV, Marushchenko LI, Sidorina YuN, Dzhedzheya GT (2016) Porphyry-epithermal systems of the Baimka Ore Zone, Western Chukotka. Smirnovskiy sbornik-2016, Maks-Press, Moscow, pp 82–115 [in Russian]

Chitalin AF, Agapitov DD, Shtengelov AR, Usenko VV, Fomichev EV (2019) The perspective for discovery of large-tonnage gold-silver deposit on the Vesenniy deposit of the Baimskaya Ore Zone, Western Chukotka. Mineral Resources of Russia: Economics and Management 2:22–29 [in Russian]

Chitalin AF, Grishin EM, Usenko VV, Fomichev EV, Chikatueva VY, Sivkov DV (2020) Structure and origin of ore stockworks of large copper, gold and tin deposits in the Kolyma-Chukotka region. Abstracts, "GeoEurasia 2020" International Geological and Geophysical Conference, Moscow. pp 27–30 [in Russian]

Chitalin AF, Baksheev IA, Nikolaev YN, Djedjeya GT, Khabibullina YN, Müller D (2022) Porphyry Cu-Au±Mo mineralization hosted by potassic igneous rocks: implications from the giant Peschanka porphyry deposit, Baimka Trend (North-East Siberia, Russia). Geol Soc Lond Spec Publ 513(1):323

Corbett GJ, Leach TM (1998) Southwest Pacific gold-copper systems: structure, alteration and mineralization. Soc Econ Geol Spec Publ 6:1–272

Crane D, Kavalieris I (2012) Geologic overview of the Oyu Tolgoi porphyry Cu-Au-Mo deposits, Mongolia. Soc Econ Geol Spec Publ 16:187–213

Franchini M, Impiccini A, Lentz DR, Rios FJ, O'Leary S, Pons J, Schalamuk AI (2011) Porphyry to epithermal transition in the Agua Rica polymetallic deposit, Catamarca, Argentina: an integrated petrologic analysis of ore and alteration paragenesis. Ore Geol Rev 41:49–74. https://doi.org/10.1016/j.oregeorev.2011.06.010

Franchini M, McFarlane C, Maydagan L, Reiche M, Lentz DR, Meinert L, Bouhier V (2015) Trace metals in pyrite and marcasite from the Agua Rica porphyry-high sulfidation epithermal deposit, Catamarca, Argentina: textural features and metal zoning at the porphyry to epithermal transition. Ore Geol Rev 66:366–387. https://doi.org/10.1016/j.oregeorev.2014.10.022

Ghaffari H, Morrison RS, de Ruijeter MA, Živković A, Hantelmann T, Ramsey D, Cowie S (2011) Preliminary assessment of the Pebble Project, Southwest Alaska. https://pebblewatch.com/wp-content/uploads/2017/05/Pebble_Project_Preliminary-Assessment-Technical-Report_February-17-2011.pdf. Accessed 15 November 2021

Gow PA, Walshe JL (2005) The role of preexisting geologic architecture in the formation of giant porphyry–related Cu–Au deposits: examples from New Guinea and Chile. Econ Geol 100:819–833

Groves DI, Santosh M, Müller D, Zhang L, Deng J, Yang LQ, Wang QF (2022) Mineral systems: their advantages in terms of developing holistic genetic models and for target generation in global mineral exploration. Geosyst Geoenviron 1:1–26. https://doi.org/10.1016/j.geogeo.2021.09.001

Kara TV, Tikhomirov PL, Demin AD (2019) New data on the age of magmatic events in the Oloy fold zone, Western Chukotka: evidence from U-Pb zircon dating. Doklady Earth Sci 489:1277–1280

KAZ Minerals (2018) Kaz Minerals press release 2018: www.kazminerals.com/our-business/baimskaya. Accessed 15 November 2021

Kirwin DJ, Forster CN, Kavalieris I, Crane D, Orssich C, Panther C, Garamjav D, Munkhbat TO, Niislelkhuu G (2005) The Oyu Tolgoi copper–gold porphyry deposits, South Gobi, Mongolia. IAOGD Guidebook Series 11:155–168

Kotova MS, Nagornaya EV, Anosova MO, Kostitsyn YuA, Baksheev IA, Nikolaev YuN, Kalko IA (2012) Dating of wall-rock alteration processes and ore-bearing granitoids of the Nakhodka ore field, Western Chukchi Peninsula. Abstracts, Geochronogical isotopic systems, methods of their study, and chronology of geological processes. V Russian Conference in Geochronogy, Moscow, 181–184 [in Russian]

Kwan K, Müller D (2020) Mount Milligan alkalic porphyry Au-Cu deposit, British Columbia, Canada, and its AEM and AIP signatures: implications for mineral exploration in covered terrains. J Appl Geophys 180:104131. https://doi.org/10.1016/j.jappgeo.2020.104131

Landtwing MR (1998) Breccias in the Cu-Mo-Au prospect of Agua Rica, Argentina: evolution of a magmatic-hydrothermal system during progressive unroofing. Unpubl. M.Sc. Thesis, ETH Zürich, Switzerland. https://doi.org/10.3929/ethz-b-000408390

Large SJE, von Quadt A, Wotzlaw JF, Guillong M, Heinrich CA (2018) Magma evolution leading to porphyry Cu-Au mineralization at the Ok Tedi deposit, Papua New Guinea: trace element geochemistry and high-precision geochronology of igneous zircon. Econ Geol 113:39–61

Loader MA, Wilkinson JJ, Armstrong RN (2017) The effect of titanite crystallisation on Eu and Ce anomalies in zircon and its implications for the assessment of porphyry Cu deposit fertility. Earth Planet Sci Lett 472:107–119. https://doi.org/10.1016/j.epsl.2017.05.010

Marushchenko LI, Baksheev IA, Nagornaya EV, Chitalin AF, Nikolaev YuN, Kalko IA, Prokofiev VYu (2015) Quartz-sericite and argillic alterations at the Peschanka Cu-Mo-Au deposit, Chukchi Peninsula, Russia. Geol Ore Deposits 57:213–225. https://doi.org/10.1134/S1075701515030034

Marushchenko LI, Baksheev IA, Nagornaya EV, Chitalin AF, Nikolaev YuN, Vlasov EA (2018) Compositional evolution of the tetrahedrite solid solution in porphyry-epithermal system: a case study of the Baimka Cu-Mo-Au trend, Chukchi Peninsula, Russia. Ore Geol Rev 103:21–37. https://doi.org/10.1016/j.oregeorev.2017.01.018

Marquez-Zavalia MF, Heinrich CA (2016) Fluid evolution in a volcanic-hosted epithermal carbonate-base-metal-gold vein system: Alto de la Blenda, Farallon Negro, Argentina. Miner Deposita 51:873–902. https://doi.org/10.1007/s00126-016-0639-y

Masterman GJ, Cooke DR, Berry RF, Walshe JL, Lee AW, Clark AH (2005) Fluid chemistry, structural setting and emplacement history of the Rosario Cu-Mo porphyry and Cu-Ag-Au epithermal veins, Collahuasi district, northern Chile. Econ Geol 100:835–862

Matteini M, Mazzuoli R, Omarini R, Cas R, Maas R (2002) The geochemical variations of the upper Cenozoic volcanism along the Calama-Olacapato-El Toro transversal fault system in the central Andes (24-S): petrogenetic and geodynamic implications. Tectonophysics 345:211–227

Maydagan L, Zattin M, Mpodozis C, Selby D, Franchini M, Dimieri L (2020) Apatite (U–Th)/He thermochronology and Re–Os ages in the Altar region, Central Andes (31°30′S), Main Cordillera of San Juan, Argentina: implications of rapid exhumation in the porphyry Cu (Au) metal endowment and regional tectonics. Miner Deposita 55:1365–1384

Müller D, Forrestal P (1998) The shoshonite porphyry Cu-Au association at Bajo de la Alumbrera, Catamarca Province, Argentina. Miner Petrol 64:47–64. https://doi.org/10.1007/BF01226563

Müller D, Groves DI (2019) Potassic igneous rocks and associated gold-copper mineralization. 5th edn. Mineral Resource Reviews. Springer Nature, Cham, 398pp

Müller D, Rock NMS, Groves DI (1992) Geochemical discrimination between shoshonitic and potassic volcanic rocks from different tectonic settings: a pilot study. Miner Petrol 46:259–289. https://doi.org/10.1007/BF01173568

Nagornaya EV (2013) Mineralogy and zoning of the Nakhodka Cu-Mo-porphyry field, Chukchi Peninsula. Ph.D. Dissertation, Lomonosov Moscow State University, Moscow [in Russian]

Nagornaya EV, Baksheev IA, Bryzgalov IA, Yapaskurt VO (2012) Minerals of the Au–Ag–Pb–Te–Se–S system of porphyry–copper–molybdenum deposits from the Nakhodka ore field, Chukchi Peninsula, Russia, Moscow. Univ Geol Bull 67:233–239. https://doi.org/10.3103/S0145875210040072

Nagornaya EV, Baksheev IA, Tikhomirov PL, Selby D (2020) The latest Aptian / earliest Albian age of the Kekura gold deposit, Western Chukotka, Russia: implications for mineralization associated with post-collisional magmatism. Miner Deposita 55:1255–1262

Nikolaev YuN, Baksheev IA, Prokofiev VYu, Nagornaya EV, Marushchenko LI, Sidorina YuN, Chitalin AF, Kal'ko IA (2016) Gold–silver mineralization in porphyry–epithermal systems of the Baimka trend, Western Chukchi Peninsula, Russia. Geol Ore Deposits 58:319–345. https://doi.org/10.1134/S107570151604005X

Nokleberg WJ, Parfenov LM, Monger JWH, Norton IO, Khanchuk AI, Stone DB, Scotese CR, Scoll DW, Fujita K (2000) Phanerozoic tectonic evolution of the Circum-North Pacific. US Geol Surv Prof Pap 1626:1–122. https://doi.org/10.3133/pp1626

Olson N, Dilles JH, Kent AJR, Lang JR (2017) Geochemistry of the Cretaceous Kaskanak batholith and genesis of the Pebble porphyry Cu-Au-Mo deposit, southwest Alaska. Amer Miner 102:1597–1621. https://doi.org/10.2138/am-2017-6053

Ossandón CG, Fréraut CR, Gustafson LB, Lindsay DD, Zentilli M (2001) Geology of the Chuquicamata mine: a progress report. Econ Geol 96:249–270

Parfenov LM (1991) Tectonics of the Verkhoyansk-Kolyma Mesozoides in the context of plate tectonics. Tectonophysics 199:319–342. https://doi.org/10.1016/0040-1951(91)90177-T

Pearce JA (1982) Trace element characteristics of lavas from destructive plate boundaries. In: Thorpe RS (ed) Andesites. Wiley, New York, pp 525–548

Pearce JA, Harris NBW, Tindle AG (1984) Trace element discrimination diagrams for the tectonic interpretation of granitic rocks. J Petrol 24:956–983

Pollard PJ, Taylor RG (2001) Paragenesis of the Grasberg Cu-Au deposit, Irian Jaya, Indonesia: results from logging Section 13. Miner Deposita 37:117–136. https://doi.org/10.1007/s00126-001-0234-7

Pollard PJ, Taylor RG, Peters L (2005) Ages of intrusion, alteration and mineralization at the Grasberg Cu-Au deposit, Papua, Indonesia. Econ Geol 100:1005–1020

Richards JP (2011) High Sr/Y arc magmas and porphyry Cu ± Mo ± Au deposits: just add water. Econ Geol 106:1075–1081. https://doi.org/10.2113/econgeo.106.7.1075

Richards JP, Razavi AM, Spell TL, Locock A, Sholeh A, Aghazadeh M (2018) Magmatic evolution and porphyry–epithermal mineralization in the Taftan volcanic complex, southeastern Iran. Ore Geol Rev 95:258–279. https://doi.org/10.1016/j.oregeorev.2018.02.018

Sidorina YN (2015) The geochemical zoning of the Nakhodka porphyry-epithermal system (West Chukotka). Moscow Univ Geol Bull 70:152–158. https://doi.org/10.3103/S0145875215020088

Sillitoe RH, Hedenquist JW (2003) Linkages between volcanotectonic settings, ore- fluid compositions, and epithermal precious metal deposits. In: Simmons SF, Graham I (eds) Volcanic, Geothermal, and Ore-Forming Fluids: Rulers and Witnesses of Processes Within the Earth. Soc Econ Geol Spec Publ 10: 315–343

Sillitoe RH, Devine FAM, Sanguinetti MI, Friedman RM (2019) Geology of the Josemaría porphyry copper-gold deposit, Argentina: formation, exhumation and burial in two million years. Econ Geol 114:407–425

Sokolov SD (2010) Tectonics of Northeast Asia: an overview. Geotectonics 44:493–509. https://doi.org/10.1134/S001685211006004X

Soloviev SG (2014) The metallogeny of shoshonitic magmatism, vol 1. Nauchny Mir, Moscow [in Russian]

Tikhomirov PL, Kalinina EA, Moriguti T, Makishima A, Kobayashi K, Cherepanova IY, Nakamura E (2012) The Cretaceous Okhotsk-Chukotka volcanic belt (NE Russia): geology, geochronology, magma output rates, and implications on the genesis of silicic LIPs. J Volcanol Geotherm Res 222:14–32. https://doi.org/10.1016/j.jvolgeores.2011.12.011

Tikhomirov PL, Prokof'ev VYu, Kal'ko IA, Apletalin AV, Nikolaev YuN, Kobayashi K, Nakamura E (2017) Post-collisional magmatism of Western Chukotka and Early Cretaceous tectonic rearrangement in Northeastern Asia. Geotectonics 51:131–151. https://doi.org/10.1134/S0016852117020054

Volchkov AG, Sokirkin GI, Shishakov VB (1982) Geological setting and ore composition of the Anyuiskoe porphyry copper deposit. Geologiya Rudnykh Mestorozhdenii 24(4):89–94 [in Russian]

Von Quadt A, Erni M, Martinek K, Moll M, Peytcheva I, Heinrich CA (2011) Zircon crystallization and the lifetimes of ore-forming magmatic hydrothermal systems. Geology 39:731–734

Winchester JA, Floyd PA (1977) Geochemical discrimination of different magma series and their differentiation products using immobile elements. Chem Geol 20:325–343. https://doi.org/10.1016/0009-2541(77)90057-2